TABLE OF CONTENTS

LIST OF TABLES

LIST OF FIGURES

3.2.P.2.2. DRUG PRODUCT

The BNT162b2 drug product is manufactured as a preservative-free, sterile, multi-dose concentrate of RNA-containing lipid nanoparticles (LNPs) formulated in phosphate-buffered saline and 300 mM sucrose at pH 7.4 to be diluted for intramuscular (IM) administration. The drug product is filled at 0.45 mL/vial (0.5 mg/mL RNA) into 2-mL glass vials which are stoppered and capped. At the administration site, the vaccine drug product is diluted with 1.8 mL of sterile 0.9% sodium chloride solution to supply 5 doses per vial at 30 µg RNA/dose.

The excipients present in the drug product were selected for the functions listed in Table 3.2.P.2.2-1. The same formulation composition has been used throughout clinical studies and for commercial production.

Table 3.2.P.2.2-1.   Function of BNT162b2 Drug Product Excipients

Excipient	Function
ALC-0315[a]	Functional lipid
ALC-0159[a]	Functional lipid
DSPC[a]	Structural lipid
Cholesterol[a]	Structural lipid
Sucrose	Cryoprotectant
Sodium chloride	Buffer component
Potassium chloride	Buffer component
Dibasic sodium phosphate, dihydrate[b]	Buffer component
Monobasic potassium phosphate[c]	Buffer component

a.   Further information regarding structure and function of the lipid excipients is provided in Section 3.2.P.2.1 Components of the Drug Product.
b.   Dibasic sodium phosphate, dihydrate is named as disodium phosphate dihydrate in the Ph. Eur.
c.   Monobasic potassium phosphate is named as potassium dihydrogen phosphate in the Ph. Eur.
Abbreviations: ALC-0315 = ((4-hydroxybutyl)azanediyl)bis(hexane-6,1-diyl)bis(2-hexyldecanoate); ALC-0159 = 2-[(polyethylene glycol)-2000]-N,N-ditetradecylacetamide; DSPC = 1,2-Distearoyl-sn-glycero-3-phosphocholine

3.2.P.2.2.1. Formulation Development

Development of a robust LNP formulation platform, that was ultimately applied to BNT162b2 drug product, was established based on formulation development studies specific to SARS-CoV-2 spike protein-encoded RNA constructs performed at Acuitas Therapeutics, along with the company's historical knowledge of LNP formulation and process development. Studies described herein were performed with available drug substance and drug product material representing the RNA platform and included both BNT162b1 and BNT162b2. As discussed in Section 3.2.P.2.2.1.3.1, once encapsulated in LNPs, BNT162b1 is considered predictive of BNT162b2 colloidal stability (size, polydispersity and % encapsulation) under freezing and temperature stress conditions.

The LNPs are composed of 2 functional and 2 structural lipid components, enabling encapsulation of the RNA payload, formation and colloidal stability of the resulting LNPs, and the transfection process.

The cationic lipid (ALC-0315) and PEGylated lipid (ALC-0159) are referred to as functional lipids. The tertiary amine group in the hydrophilic head of ALC-0315 electrostatically interacts with the anionic backbone of the RNA to condense the RNA molecule during the encapsulation process. The functional performance of ALC-0315 was tested in vivo using systemic administration of RNA-containing LNPs. ALC-0315 has an apparent pKa of 6.1 that complies with a known optimum for cationic lipids in LNP[1]. LNPs are taken up in an ApoE-dependent mechanism[2] and this mode of action was confirmed for the initial formulation. Upon completion of the initial screening cycle using the systemic route of administration, the activity of the actual lead LNP comprising ALC-0315 was then confirmed for the intramuscular route of administration. It was also demonstrated that the uptake on the intramuscular route is ApoE dependent, which permits bridging across these modalities. The PEGylated lipid (ALC-0159) predominantly localizes at the surface of the LNP, forming a steric barrier to surfaces of surrounding LNPs thus contributing to colloidal stability. As PEGylation is known to inhibit cellular uptake, a diffusible PEG lipid was chosen. The rate constant for the diffusion of ALC-0159 relates to the size of the apolar moiety[3] and is optimized to retain the PEG corona during storage and PEG diffusion upon administration.

The lipids DSPC and cholesterol are referred to as structural lipids and comply with standard LNP designs.

The LNPs were suspended in phosphate buffered saline (PBS) as the formulation vehicle during initial development. Sucrose was added as a cryoprotectant to enable storage as a frozen drug product.

During the initial formulation development process, BNT162b2 stability was evaluated using assays that addressed the critical attributes required for determination of safety and potency of the drug product. The critical attributes related to LNP formation and payload delivery are primarily nanoparticle size, encapsulation efficiency, and an in vivo study to demonstrate potency of the nanoparticles, using a luciferase-encoded RNA as a surrogate. For manufacturing support, BNT162b2 drug product was evaluated primarily for size, polydispersity, and the extent of RNA exposure (% Encapsulation) of the LNPs to determine colloidal stability, as well as RNA integrity (by capillary gel electrophoresis) and lipids content to determine the chemical stability of the components.

Table 3.2.P.2.2-2 contains a list of the formulation development studies that were conducted during BNT162b2 development and links to the descriptions of each study within this section.

Table 3.2.P.2.2-2.   BNT162b2 Formulation Development Studies

Development Study	Study Summary/Outcome	Location
Initial LNP formulation development at Acuitas Therapeutics	Screening studies leading to the selection of the LNP formulation and confirmation of in vivo activity of the RNA payload.	3.2.P.2.2.1.1
Formulation of the drug product[a]	Studies supporting the drug product formulation process.	3.2.P.2.2.1.1.3.3
Drug product stability – effect of freeze and thaw, frozen and liquid storage	Development stability study data supporting initial assessment of storage stability. Determination of Tg', effect of freeze and thaw on drug product during manufacturing operations and stability upon long term storage.	3.2.P.2.2.1.3 3.2.P.2.2.1.4
Excess volume in vial[a]	Rationale for an excess volume in the vial after dilution with 1.8 mL of sterile 0.9% NaCl (saline).	3.2.P.2.2.1.5
Physicochemical and Biological Properties	Physicochemical properties of the drug product.	3.2.P.2.2.3
Enhanced analytical characterization	Enhance characterization and additional properties of the BNT162b2 drug product are described.	3.2.P.2.2.3.4

a. Study performed with BNT162b1 as a surrogate for BNT162b2 based on LNP size, LNP polydispersity and % RNA encapsulation.

Given that many of the analytical methods were still in development when the studies were conducted, the analytical results reported throughout this section reflect the status of the methods at the time of the studies. For example, most data were generated before the formal validation and the formal establishment of quantitation limits (QL) of the corresponding assays. Results lower than the formally validated QL may be presented in this section as they were originally reported. Table 3.2.P.2.2-3 shows the methods that were used to assess BNT162b2 quality attributes (QA) during development, and the corresponding methods that are intended to be used for commercial release and stability testing.

Table 3.2.P.2.2-3.   Analytical Methods and Quality Attributes Assessed During BNT162b2 Drug Product Development

Quality Attribute Assessed	Development Method	Release/Stability Method
Appearance	Visual Inspection	Visual inspection
Appearance (Visible Particulates)	Appearance, clarity, Ph. Eur. 2.9.20	Appearance, clarity, Ph.Eur. 2.9.20
Lipid Identities	HPLC-CAD	HPLC-CAD
ALC-0315 content	HPLC-CAD	HPLC-CAD
ALC-0159 content	HPLC-CAD	HPLC-CAD
DSPC content	HPLC-CAD	HPLC-CAD
Cholesterol content	HPLC-CAD	HPLC-CAD
RNA identification	Capillary gel electrophoresis	RT-PCR
RNA integrity	Capillary gel electrophoresis	Capillary gel electrophoresis
RNA encapsulation	Fluorescence assay	Fluorescence assay
RNA content	Fluorescence assay	Fluorescence assay
LNP size	Dynamic light scattering	Dynamic light scattering
LNP polydispersity	Dynamic light scattering	Dynamic light scattering
pH	Ph. Eur. 2.2.3	USP<791>, Ph. Eur. 2.2.3
Osmolality	Ph. Eur. 2.2.35	USP<785>, Ph. Eur. 2.2.35
Subvisible particles	Ph. Eur. 2.9.19	USP<787>, Ph. Eur. 2.9.19
Bacterial Endotoxins	Ph. Eur. 2.6.14	USP<85>, Ph. Eur. 2.6.14
Sterility	Ph. Eur. 2.6.1	USP<71>, Ph. Eur. 2.6.1

3.2.P.2.2.1.1. Lipid Nanoparticle Screening Process

Formulation development began with screening of lipid nanoparticles. This involved incorporation of the novel lipids into LNPs encapsulating RNA and then submission to a screening process which included pilot formulation and physical characterization to determine suitability for in vivo testing and activity determination in a murine model of RNA expression.

During pilot formulation, candidate cationic lipids were formulated with RNA encoding for luciferase and other component lipids in a standardized composition which comprised the cationic lipid (ALC-0315, ALC-0218, etc.), a PEGylated lipid (ALC-0159), DSPC and cholesterol. The use of RNA coding for luciferase allowed for visual assessment of expression and translation in model systems. Results of these studies led to the selection of ALC-0315.

The criteria to determine suitability for in vivo screening at this initial stage were the minimum encapsulation of RNA, the apparent pKa as well as LNP size and LNP polydispersity.

RNA molecules that are not fully encapsulated and protected by the LNP are considered inactive, as they are exposed to nucleases and further degradation after administration. RNA must be sufficiently intact to be successfully translated to the target protein, hence a minimum level of encapsulation efficiency needs to be achieved for a candidate RNA-LNP system. This minimum threshold is approximately 70% based on Acuitas Therapeutics general experience.

The hypothesized mechanism of delivery for RNA/LNPs involves binding of endogenous proteins to the LNP surface, which then act as ligands to facilitate receptor mediated endocytosis, followed by interaction with the interior of the endosome to trigger release of the RNA to the cytoplasm. ApoE has been identified as co-factor for LNP uptake and confirmed as sufficient to rescue uptake of the LNP in ApoE-deficient mice for both the systemic and intramuscular routes of administration. The LDL receptor is thought to be the cellular receptor for ApoE-decorated LNP, which is linked to clathrin-mediated endocytosis[2].

Low surface charge in the blood compartment is considered critical to avoid nonspecific binding to and eventual aggregation with serum components or cellular surfaces which relates to toxicity. Conversely, a high cationic surface charge is required for the interaction with the endosomal membrane and eventual fusion and endosome escape. This dual nature of the LNP is achieved through ionizable cationic lipids, and successful compounds generally possess an apparent pKa (i.e., pKa as measured when part of an LNP as opposed to free in solution) within a target range of 5-7, preferably between 6 and 6.5[4]. Therefore, novel cationic lipids are formulated as LNP and the apparent pKa is determined as an important selection criterion.

Historical experience[2] with similar systems has indicated that well formed LNP are generally homogeneous with relatively narrow size distribution and a mean size that is within a

preferred range. The preferred range is generally below 200 nm but LNP outside this range may be accepted for screening purposes to prevent exclusion of compound classes that can later be optimized with respect to this parameter. The size range is thought to relate to the mode of action that involves the clathrin pathway[5].

3.2.P.2.2.1.1.1. Lipid Components

The formulation composition consists of four lipid components as described in Section 3.2.P.2.1 Components of the Drug Product. The function and rationale for each of the lipid components is briefly described.

Cationic Lipid (ALC-0315)

The ionizable cationic lipid is the most important LNP component for providing successful delivery of RNA. Its properties are critical to the self-assembly process of the particle itself, the ability of the LNP to be taken up into cells, and the escape of the RNA from the endosome.

PEGylated Lipid (ALC-0159)

The polyethylene glycol (PEG) lipid conjugate (PEGylated lipid) inserts itself in the outer lipid bilayer of the LNP. The PEG domain provides a steric barrier to interactions with surfaces or other LNP that may otherwise result in particle fusion during storage.

Phospholipid (DSPC)

The phospholipid component balances the non-bilayer propensity of the cationic lipid. The combination of the structural lipid DSPC and cholesterol is established for LNP as a platform and is also used in Onpattro®, a marketed product.

Sterol Lipid (Cholesterol)

Cholesterol supports bilayer structures in the LNP by acting as a stabilizing intermediary in the interactions between the conventional phospholipid and the structurally novel cationic lipid and provides mobility of the lipid components within the LNP structure. Cholesterol is selected over other sterol lipids because it is considered safe as it is naturally occurring and ubiquitous.

3.2.P.2.2.1.1.2. Selection of ALC-0315 Formulation

The LNP delivery system was developed to effectively and safely deliver therapeutic nucleic acids into the cytosol of various cell types after local administration in vivo. This early formulation work, using a mouse model, was performed with several promising LNP formulations and surrogate RNA coding for luciferase. The aim of the experiments was to correlate the effect of different ionizable cationic lipids on the efficacy of RNA delivery by LNPs in vivo. In this screening study, the RNA payload was kept constant (weight). The lipids, for which the number of molecules is the important factor for comparison, were used at μmolar concentrations. Formulations were compared with respect to RNA encapsulation efficiency, apparent pKa, LNP size and polydispersity.

Among the screened cationic lipids, ALC-0315 exhibited suitable physical characteristics regarding particle size, homogeneity, and RNA encapsulation efficiency, as shown in Table 3.2.P.2.2-4 for two independent pilot batches.

Table 3.2.P.2.2-4.   **Physical Characterization of ALC-0315 Pilot Formulation**

ALC-0315 Pilot Formulation	Apparent pKa	Mean LNP Size (nm)	RNA Encapsulation (%)	mRNA:Total Lipid (wt/µmol)	In Vivo Activity Relative to Benchmark[a]
Batch 1	6.09	64	83	0.030	2.20
Batch 2		66	87	0.032	2.55

a.   Fold increase in luciferase expression

Based on this, the ALC-0315/ALC-0159/DSPC/CHOL prototype was submitted for in vivo screening. The results presented in Figure 3.2.P.2.2-1 and Figure 3.2.P.2.2-2 summarize the in vivo testing of two independent pilot batches using luciferase (Luc) RNA. The results demonstrate improved potency of the ALC-0315 prototype as compared to an internal benchmark (ALC-0218). Based on these studies, ALC-0315 was identified as a highly potent cationic lipid and brought forward for further product development.

Figure 3.2.P.2.2-1.   **ALC-0315 Activity in the Screening Process – Batch 1**
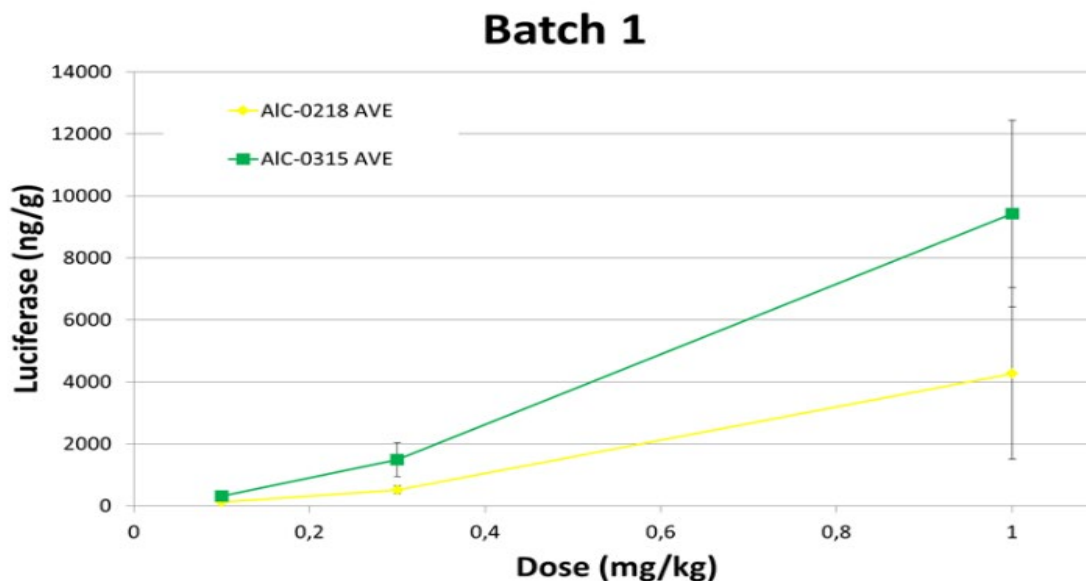
Figure 3.2.P.2.2-2.   ALC-0315 Activity in the Screening Process - Batch 2
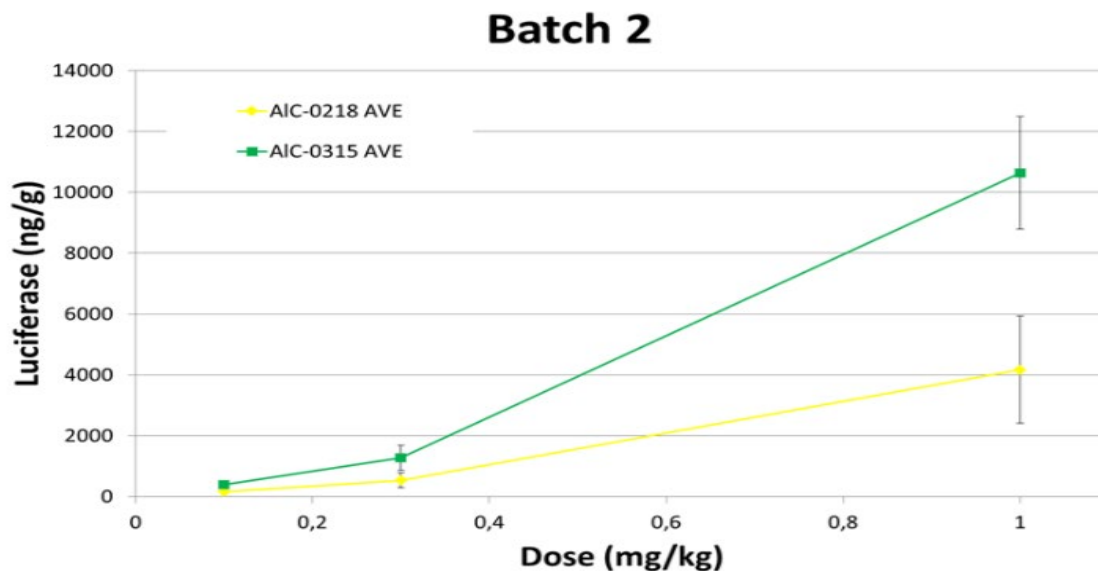
The formulation screening procedure described above involves intravenous (IV) administration resulting in delivery primarily to the liver. The mechanism of LNP uptake into hepatocytes is driven by binding of endogenous apolipoproteins to the LNP followed by receptor-mediated endocytosis, e.g., through low-density lipoprotein receptors. In order to investigate whether the same mechanism is involved for intramuscular (IM) administration, Luc RNA-containing LNPs comprising ALC-0315 were injected intravenously (0.3 mg/kg) and intramuscularly (0.2 mg/kg) into Apolipoprotein E (ApoE) knockout (KO) mice in the presence (KO+) or absence (KO-) of recombinant human ApoE3. As control, wild-type (WT) C57Bl/6 mice were also treated by the different routes of administration. RNA-LNP were pre-incubated with recombinant human ApoE3 (1 mg encapsulated mRNA with 1 mg ApoE3) for 1 hour at room temperature (RT) prior to administration. Luciferase expression was detected using Xenolight D-Luciferin Rediject at 4, 24, 72, and 96 hours post administration.

When mice were administered intravenously, Luc expression was detected in the WT C57Bl/6 mice. In the ApoE KO mice Luc expression was significantly reduced. However, when preincubated with exogenous ApoE the expression of Luc was recovered to similar expression levels as WT mice as measured by Luc expression 4 hours post-injection. IM administration was also ApoE-dependent with significant reduction in activity in ApoE KO animals (Figure 3.2.P.2.2-3).

Figure 3.2.P.2.2-3.   Luciferase Expression after IV and IM Administration in WT or ApoE KO C57Bl/6 Mice in the Presence (KO+) or Absence (KO) of ApoE at 4 Hours Post Administration
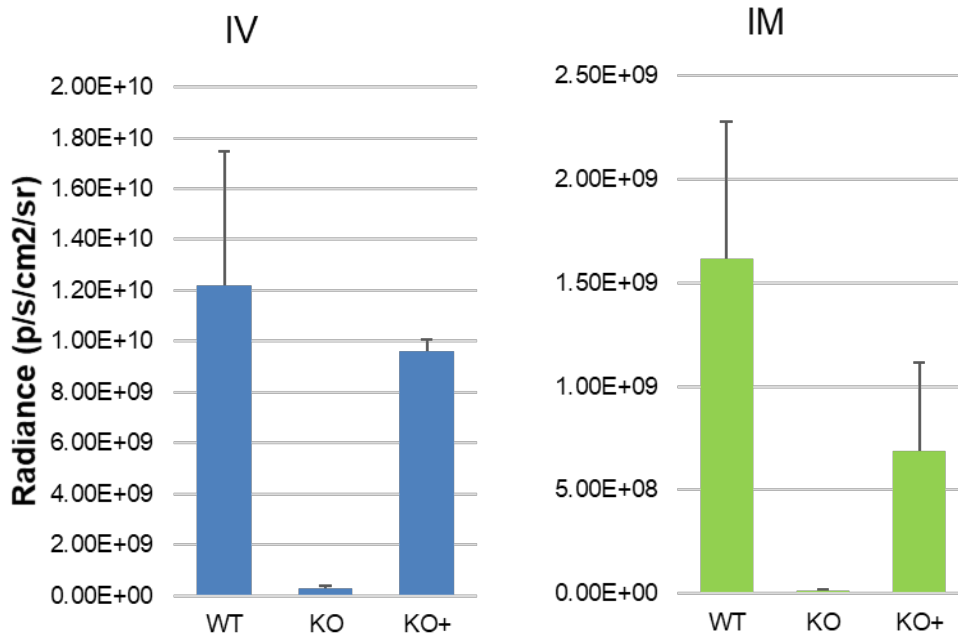
In vivo Luc expression experiments using mouse models showed that similar mechanisms are involved in the uptake of RNA-LNP for IM administration as for IV administration as shown in Figure 3.2.P.2.2-4 by Luc expression at 4, 24, 72 and 96 hours after administration. This is true for hepatocytes as well as for the cells local to the administration site.

Figure 3.2.P.2.2-4. **Luciferase Expression Monitored at 4, 24, 72 and 96 Hours on Right (site of injection), Dorsal (site of injection) and Ventral (drainage to the liver) Sides after IM Administration in WT or ApoE KO C57Bl/6 Mice in the Presence or Absence of ApoE3**
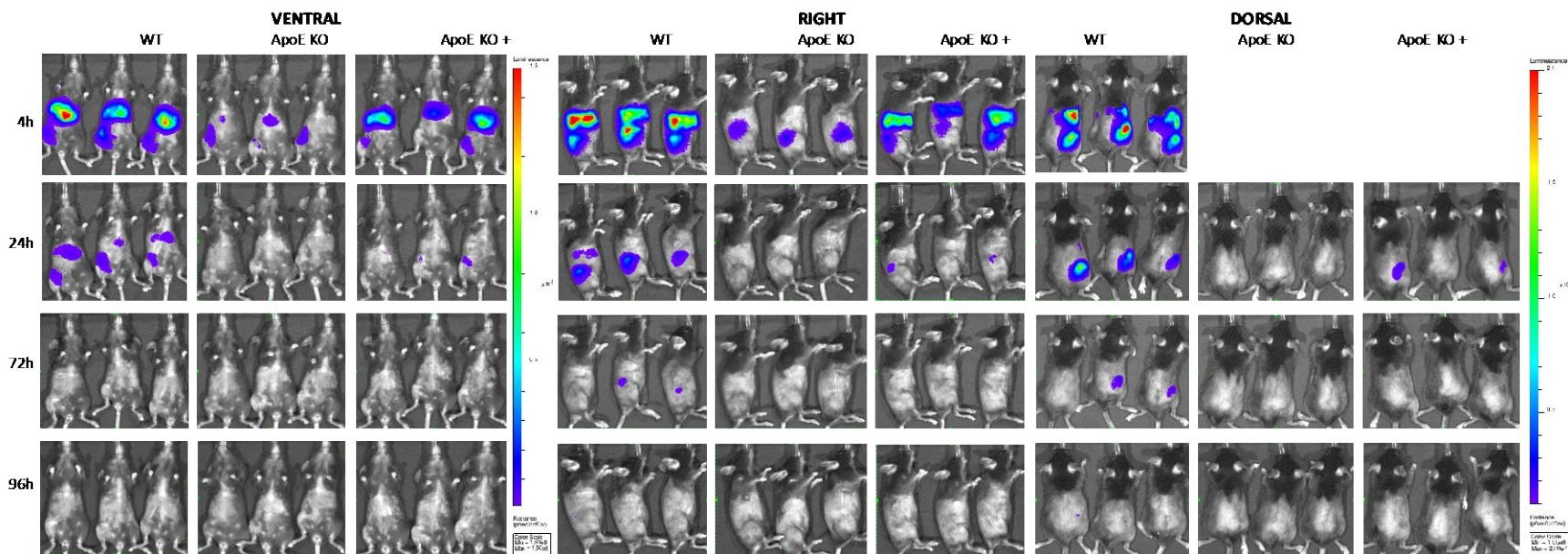
Abbreviations: IM = Intramuscular; WT = Wild Type; KO = Knockout; ApoE = Apolipoprotein E;

In vivo experiments after IM administration of the final ALC-0315/ALC-0159/DSPC/CHOL LNP at molar ratio 47.5/10/40.7/1.8, confirmed expression of mRNA for this route of administration.

The conclusion of these studies was that the LNP formulation incorporating the lipids ALC-0315, ALC-0159, DSPC, and cholesterol is appropriate for the intended use as an intramuscular injection.

3.2.P.2.2.1.1.3. Establishing In Vitro and In Vivo Correlation

While in vivo animal experiments were used in early development, for example, in previously described formulation selection studies, they are not amenable for routine characterization of the BNT162b2 drug product. Therefore, an in vitro expression (IVE) assay was developed to measure the expression of SARS-CoV-2 spike antigen from cultured cells incubated with the BNT162b2 drug product. A study was performed to evaluate the correlation between in vitro expression of the SARS-CoV-2 spike antigen and the antigen-binding IgG and SARS-CoV-2 neutralizing responses of mice immunized with the DP. The study also evaluated the correlation between IVE and the percentage of BNT162b2 RNA that is both capped and full length.

3.2.P.2.2.1.1.3.1. Preparation of Drug Substance and Drug Product Materials with Different Degrees of Capping and Integrity

To provide test materials with a wide range of in vitro and in vivo activity, capped and uncapped RNA BNT162b2 drug substance (DS) samples were produced. In addition, the degraded DS sample was generated by incubating intact RNA DS at 65 °C for 3.5 days. To create preparations with a variety of levels of capping and integrity, drug substances with high integrity and low integrity were mixed, and drug substances with and without cap were mixed. The RNAs were then formulated into LNPs to produce drug products (DPs). The abundance of 5'-Cap levels of the RNA in the DP varied from 0-67%. The RNA integrity measured by capillary gel electrophoresis varied from 1-71%. Because mRNA must be both capped and intact to express protein, the capped-intact RNA integrity was determined for each test preparation (Capped-intact RNA (%) = RNA Integrity (%) x 5'-Cap (%)). The capped-intact RNA integrity values of the RNA in the DPs varied from 0-43%.

3.2.P.2.2.1.1.3.2. Analytical Characterization of Drug Substance and Drug Product

Capillary Gel Electrophoresis (Fragment Analyzer)

The RNA integrity is assessed using a capillary gel electrophoresis-based (CGE) method, also called the Fragment Analyzer (FA) method, to separate components based on the differential migration of RNA of different molecular size in an applied electric field. An intercalating dye binds to RNA and associated fragments during migration allowing for fluorescence detection. RNA integrity is determined by the relative percent peak area for the intact (main) electropherogram peak.

5'-Cap Analysis (LC-MS)

The percentage of capped RNA is measured by an RNase H based assay. RNA samples are annealed to a customized biotinylated nucleic acid probe binding close to the 5′ end of the RNA, and RNase H is used to digest the RNA-probe complex. This gives a short fragment corresponding to the 5′ part of the RNA. Streptavidin-coated spin columns or magnetic beads are used for sample clean-up, and then the purified samples with the 5′ part of the RNA are analysed by LC-MS. The capped and non-capped species are identified by the observed mass values, and their MS signals are used to calculate the percentage of capped RNA.

In Vitro Spike Protein Expression (IVE)

RNA containing lipid nanoparticles (LNPs) at a non-saturating RNA dose level of 100 ng is added to HEK-293T cells. Protein expression is measured using an anti-spike protein receptor binding domain (RBD) rabbit monoclonal antibody. Prior to analysis by flow cytometry, cells are labeled with a Live/Dead dye and the percent of live cells (to eliminate background signal) expressing spike protein is enumerated. Expression is measured by quantifying the number of cells that have a positive signal for bound anti-RBD antibody.

3.2.P.2.2.1.1.3.3. Mouse Immunization

Groups of 10 female, Balb/c mice (Jackson Laboratories) were 9-11 weeks old at the commencement of the study. DP at the 0.2 μg dose level or saline diluent control was injected IM with blood collected on Day 21 by the submandibular route. A naïve cohort served as an untreated control. The mouse study was conducted according to Pfizer local and global institutional animal care and use committee guidelines at an Association for Assessment and Accreditation of Laboratory Animal Care International–accredited facility.

3.2.P.2.2.1.1.3.4. Serology

The S-binding antibody response elicited by mouse immunization was assessed by a S1-binding IgG Luminex assay. Serum IgG bound to S1-coated microspheres was detected with a R-phycoerythrin labeled secondary antibody and fluorescent signal read with a Luminex FLEXMAP 3D reader. The data were analyzed using a custom SAS application, which uses a log/log linear regression model of the standard curve based on a RBD-specific mouse monoclonal antibody to interpolate antigen-specific antibody concentrations (μg/mL) from median fluorescent intensity. The functional antibody response was determined with a SARS-CoV-2 neutralization assay that assessed the ability of post-immunization sera to inhibit infection of a Vero CCL81 monolayer by a SARS-CoV-2 strain (USA_WA1/2020) that expresses a fluorescent marker[6]. This reporter virus generates similar plaque morphologies and indistinguishable growth curves from wild-type virus[7]. Infected cells were detected by a Cytation 7 Cell Imaging Multi-Mode Reader (Biotek) with Gen5 Image Prime version 3.09. Titers were calculated in GraphPad Prism version 8.4.2 by generating a 4-parameter (4PL) logistical fit of the percent neutralization at each serial serum dilution. The 50% neutralization titer was reported as the interpolated reciprocal of the dilution yielding a 50% reduction in fluorescent viral foci.

3.2.P.2.2.1.1.3.5. Correlating In Vitro Expression with Elicted Mouse Antigen-Binding IgG and Neutralization Responses and with Capped-Intact Integrity

Scatter plots of S1-binding IgG concentrations (left panel) and 50% SARS-CoV-2 neutralizing titers (right panel) in mouse sera obtained 21 days after immunization with BNT162b2 DP preparations as a function of IVE from HEK-293T cells incubated with the DP preparations are presented in Figure 3.2.P.2.2-5. Each graph also displays the capped-intact integrity of RNA in the BNT162b2 DP preparations as a function of IVE. The S1-binding IgG response correlated well with IVE ($R^2 = 0.75$). The SARS-CoV-2 50% neutralizing response correlated with IVE ($R^2 = 0.52$). Capped-intact integrity correlated strongly with IVE ($R^2 = 0.91$).

Figure 3.2.P.2.2-5.   Correlation of S1-binding IgG Responses and Neutralization Titers in Mice at Day 21 with In Vitro Expression
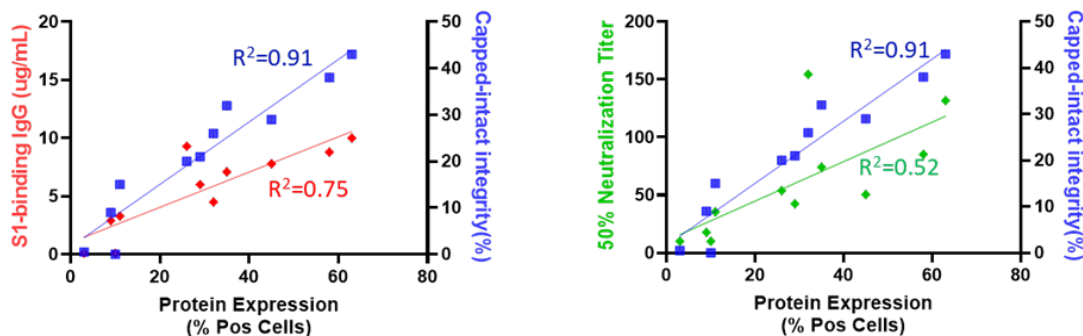
3.2.P.2.2.1.1.3.6. Conclusion

The data demonstrate that BNT162b2 drug product in vitro expression correlates with antigen-binding antibody responses and SARS-CoV-2 neutralizing responses in mice immunized with the drug product. The in vitro expression also correlates with capped-intact RNA integrity. The IVE assay has been routinely used in the development of the BNT162b2 vaccine and has been optimized and validated for DP release and stability testing (reference Section 3.2.P.5.2 Cell-based Flow Cytometry and Section 3.2.P.5.3 Cell-based Flow Cytometry).

3.2.P.2.2.1.2. Formulation of the Drug Product

Parameters such as the buffer strength, N/P ratio (the molar ratio of the amine in the cationic lipid (N) to the phosphate in anionic phosphodiester backbone of RNA (P)) and mixing rate of organic and aqueous components have been optimized in order to enable efficient RNA encapsulation.

RNA Stock Solution

The RNA is prepared in an aqueous solution prior to mixing. Efficient encapsulation of nucleic acid payload upon mixing requires a charge-based interaction between the phosphate backbone of the nucleic acid and the amine moiety of the ALC-0315 cationic lipid. To ensure this coulombic interaction, the pH of the mixing solution is controlled with an appropriate

aqueous buffer at a pH that maintains ionization of both the nucleic acid backbone and the cationic lipid. An optimum between the pKa of the nucleic acid backbone (~2) and the pKa of ALC-0315 is found at pH 4, which is achieved by using RNA dissolved in citrate buffer at pH 4.0 where the time of RNA exposure prior to mixing is minimized.

Table 3.2.P.2.2-5 provides data with respect to buffer strength showing no significant difference in LNP size, LNP polydispersity and % RNA encapsulation for LNP formulated either with RNA in 50 mM or 10 mM citrate buffer. This data indicates that 10 mM is sufficient and therefore 50 mM citrate provides excess buffering capacity for process robustness without any negative effect. Therefore, a citrate buffer concentration of 50 mM was selected to control pH in the presence of the nucleic acid with some level of excess to provide robustness.

Table 3.2.P.2.2-5.   Effect of Buffer Strength on the ALC-0135 Formulation

Buffer	Total Mixing Flow Rate (mL/min)	Post Mixing Incubation Temperature	LNP Size (nm)	LNP PDI	RNA Encapsulation (%)
50 mM Citrate, pH 4.0	24	RT	68	0.088	83
		37 °C	69	0.063	83
10 mM Citrate, pH 4.0	24	RT	68	0.133	80
		37 °C	66	0.086	85

Abbreviations: LNP = lipid nanoparticle; PDI = Polydispersity

Lipid Stock Solution

The lipid stock solution can be prepared either by directly weighing lipid components in the target proportions to a single container and dissolving in an appropriate solvent, or by volumetrically combining high concentration (10-20 mg/mL) solutions of individual lipid components to achieve the same target proportions and final total lipid concentrations. For large scale production the lipid components are weighed and added directly to ethanol in the heated (35 °C setpoint) organic phase vessel prior to mixing. Ethanol is chosen as a solvent that will support dissolution of all the lipid components and has a minimal toxicity risk for any residual solvent remaining after completion of manufacturing.

Stock Solution Concentrations

The concentrations of the stock solutions for mixing are calculated based on a target ratio of cationic lipid to RNA (ratio of organic to aqueous component) and a target output lipid concentration relative to RNA concentration.

The ratio of cationic lipid to RNA for the ALC-0315 formulation is based on historical experience with similar lipids and nucleic acids and is specified in terms of an N/P ratio where N represents the molar ratio of the ionizable amine in ALC-0315 and P represents the phosphate in the anionic phosphodiester backbone of RNA.

Efficient encapsulation requires that there is sufficient cationic lipid to interact with the entire phosphodiester backbone. Furthermore, there must also be sufficient free cationic lipid to

effect endosomal release once administered which requires a molar excess of cationic lipid relative to the nucleotides. The target N/P ratio has not changed throughout development of the upscale process.

As shown in Table 3.2.P.2.2-6, reasonable balance was found at an N/P ratio of 6.3, where neither LNP polydispersity and RNA encapsulation nor the LNP size is significantly affected.

Table 3.2.P.2.2-6.   N/P Ratio Variants for ALC-0315 Formulation

N/P Ratio	LNP Size (nm)	LNP PDI	RNA Encapsulation (%)
3.2	78	0.067	88
6.3	73	0.093	87
32	93	0.088	92

Abbreviations: LNP = lipid nanoparticle; PDI = polydispersity

The LNPs effectively form as a colloid from precipitation of the lipid components upon rapid change of the solubility characteristics of the lipids in the solution when the aqueous component is introduced; hence the ratio of organic to aqueous component is of high importance. The proportion of organic component in the mixed solution must be sufficiently low to induce this colloidal precipitation with kinetics that are fast enough to support nanoscale particles. ALC-0315 formulations are generally prepared with final ethanol concentration of 25% (v/v) which corresponds to a mixing ratio of 3:1. This ratio is in the center of what is considered a functional range and as such it provides a margin of robustness with respect to forming LNP systems.

Mixing assembly

The components of the mixing system are readily available as standard parts in high-performance liquid chromatography (HPLC) and other fluidic devices. The mixing dynamics are controlled by the orifices at the outlet of each stream and by the internal diameters of the tubing.

Homogenous lipid nanoparticle formation with appropriately small sizes requires fast and efficient mixing of the aqueous and organic components. The flow rates of the organic and aqueous components are controlled independently by two separate pumps. The pump speeds are related to each other by the target final organic component concentration (25% ethanol) and by the same ratio as the stock solution volumes (3 aqueous: 1 organic) in order to continuously provide the same step dilution at the mixing interface for the entire mixing process. At lower flow rates (8 and 12 mL/min), particles had larger sizes and higher polydispersity characteristics with low RNA encapsulation efficiency while at the higher flow rate (60 mL/min) the LNP size and LNP polydispersity were also higher (Table 3.2.P.2.2-7). Therefore, preliminary flow rates of 18 to 40 mL/min were chosen for this formulation. Mixing apparatus dimensions have changed for scale up to the commercial process (termed "Upscale" process) which necessitates a change in the target for flow rate. During scale up, flow rates were changed to 120:40 mL/min (total 160 mL/min) for the "Classical" process and 360:120 mL/min (total 480 mL/min) for the "Upscale" process

(Section 3.2.P.2.3 Process Development and Characterization, subsection 3.2.P.2.3.6.3 Development of LNP Manufacturing "Classical Process" and "Upscale Process.").

Table 3.2.P.2.2-7.   Effect of Mixing Rate on ALC-0315 Formulations

Total Mixing Flow Rate (mL/min)	LNP Size (nm)	LNP PDI	RNA Encapsulation (%)
8	130	0.080	50
12	89	0.070	73
18	82	0.052	85
24	77	0.045	89
40	70	0.070	91
60	125	0.191	87

Abbreviations: LNP = lipid nanoparticle; PDI = polydispersity

Final Process Steps

Once the particles have formed, the ethanol component and low pH condition are no longer necessary and require removal. This was initially achieved with dialysis which later changed to tangential flow filtration for the final formulation steps.

In order to provide an isotonic drug product that could be further diluted for administration, the standard phosphate-buffered saline was chosen for the final formulation. In order to support frozen storage to ensure stability of the drug product, a cryoprotectant was required. Sucrose is generally used for this purpose and was added to the formulation at a final concentration of 300 mM. The final formulation is achieved by formulating the RNA-containing LNP concentrate at 0.5 mg/mL (RNA) with phosphate-buffered saline and 300 mM sucrose at pH 7.4.

Studies have been initiated to determine the stability at frozen, refrigerated and ambient temperatures for BNT162b2 drug product (Section 3.2.P.8 Stability).

3.2.P.2.2.1.3. Stability of the Drug Product

BNT162b1 was initially designated as a commercial candidate. Process development studies were performed using BNT162b1 and a development stability study was initiated. BNT162b2 has since been identified as the commercial candidate, and since BNT162b1 and BNT162b2 are similar constructs (BNT162b1 is also a RNA construct but encodes for only the spike protein receptor binding domain instead of the full spike protein encoded by BNT162b2), it was considered whether available data on BNT162b1 could provide some assurance of formulation stability and support for the development studies that were in progress prior to availability of BNT162b2 for development. As the difference between the constructs is the length of the RNA (BNT162b2 RNA: 4283 nucleotides; BNT162b1 RNA: 1262 nucleotides) it is reasonable that once encapsulated in the LNP, freezing and temperature stress might be expected to impact LNP size, LNP polydispersity and % RNA encapsulation in a similar fashion for both constructs. However, other attributes related to RNA integrity may not be as predictive. Therefore, physicochemical and colloidal data available for the BNT162b1 drug product are discussed for comparative purposes. Limited

data for the BNT162b2 drug product are shown below in Section 3.2.P.2.2.1.3.2 and in Section 3.2.P.8.3 Long-Term and Section 3.2.P.8.3 Accelerated.

Results of the development stability studies for BNT162b1 and BNT162b2 are discussed in Section 3.2.P.2.2.1.3.1 and Section 3.2.P.2.2.1.3.2 respectively.

3.2.P.2.2.1.3.1. BNT162b1 Drug Product Development Stability

BNT162b1 drug product was manufactured by Acuitas Therapeutics and shipped at 2-8 °C to Pfizer Andover, where the drug product was filled at 0.5 mL per 2 mL vial. Vials were stoppered and capped and stored at -70±10 °C, -20±5 °C, 2-8 °C and 25±2 °C for up to 4 weeks. As the study was discontinued, results for BNT162b1 are discussed to the 1-month timepoint.

Results of these studies using the BNT162b1 drug product indicate that there was no change to quality attributes related to LNP size, LNP polydispersity or % RNA encapsulation as well as other attributes considered relevant to BNT162b2 when the drug product was stored at the recommended frozen temperature of -70±10 °C for up to 1 month, and accelerated temperatures of 2-8 °C for up to 2 weeks and 25±2 °C for up to 10 days. There was a small increase in LNP size by dynamic light scattering when the drug product was subjected to 3x freeze/thaw cycles after 2 weeks at 2-8 °C and 10 days at 25±2 °C. There was also a small increase in LNP size when the drug product was subjected to the accelerated frozen temperature of -20±5 °C which is above the T_g' for BNT162b2 drug product (Section 3.2.P.2.2.3.3). These results suggest that these slight changes in LNP size could occur for the BNT162b2 drug product under the same storage conditions. Results are shown in Table 3.2.P.2.2-8, Table 3.2.P.2.2-9, Table 3.2.P.2.2-10, and Table 3.2.P.2.2-11.

Table 3.2.P.2.2-8. Frozen Stability of BNT162b1 at -70±10 °C for 4 Weeks

Quality Attribute	T0[a]	7 days	4 weeks
Appearance (Color)	≤Y4	≤Y5	≤Y4
Appearance (Clarity)	>REF IV	>REF IV	>REF IV
Appearance (Visible Particles)	EFVP	EFVP	EFVP
pH	6.9	NT	NT
RNA Content (Ribogreen) (μg/mL)	442	442	448
RNA Encapsulation (Ribogreen) (%)	90	88	89
ALC-0315 Content (mg/mL)	7.79	7.31	7.53
ALC-0159 Content (mg/mL)	0.95	0.87	0.97
DSPC Content (mg/mL)	1.64	1.53	1.59
Cholesterol Content (mg/mL)	3.31	3.05	3.12
LNP Size (DLS) (nm)	76	76	74
LNP Polydispersity (DLS)	0.164	0.247	0.204

a. T0 shared for -20±5 °C and -70±10 °C
Abbreviations: EFVP = essentially free of visible particulates; NS = not scheduled; LNP = lipid nanoparticle; DLS = dynamic light scattering; NT = not tested

Table 3.2.P.2.2-9.   Frozen Stability of BNT162b1 at -20±5 °C for Two Weeks

Quality Attribute	T0ᵃ	7 days	2 weeks
Appearance (Color)	≤Y4	≤Y5	≤Y4
Appearance (Clarity)	>REF IV	>REF IV	>REF IV
Appearance (Visible Particles)	EFVP	EFVP	EFVP
pH	6.9	6.9	6.9
RNA Content (Ribogreen) (µg/mL)	442	438	425
RNA Encapsulation (Ribogreen) (%)	90	88	87
ALC-0315 Content (mg/mL)	7.79	7.37	7.04
ALC-0159 Content (mg/mL)	0.95	0.88	0.85
DSPC Content mg/mL)	1.64	1.55	1.45
Cholesterol Content (mg/mL)	3.31	3.09	2.96
LNP Size (DLS) (nm)	76	88	91
LNP Polydispersity (DLS)	0.164	0.237	0.262

a. T0 shared for -20±5 °C and -70±10 °C
Abbreviations: NS = not scheduled; EFVP = essentially free of visible particulates; FA = fluorescence assay;
LNP = lipid nanoparticle; DLS = dynamic light scattering

Table 3.2.P.2.2-10.   Liquid Stability of BNT162b1 at 2-8 °C including 3x Freeze and Thaw at 2 Weeks

Quality Attribute	T0ᵃ	7 days	10 days	2 weeks	2 weeks (3X F/T)	4 weeks
Appearance (Color)	≤Y4	≤Y5	≤Y4	≤Y4	≤Y4	≤Y4
Appearance (Clarity)	>REF IV	>REF IV	>REF IV	>REF IV	>REF IV	>REF IV
Visible Particles	EFVP	EFVP	EFVP	EFVP	EFVP	EFVP
pH	6.9	7.0	6.9	6.9	6.9	6.9
RNA Content (Ribogreen) (µg/mL)	432	438	442	424	431	440
RNA Encapsulation (Ribogreen) (%)	91	92	90	88	86	89
ALC-0315 Content (mg/mL)	7.92	7.27	7.05	7.22	7.33	7.50
ALC-0159 Content (mg/mL)	0.96	0.91	0.85	0.85	0.87	0.98
DSPC Content (mg/mL)	1.67	1.52	1.45	1.48	1.48	1.60
Cholesterol Content (mg/mL)	3.36	3.02	2.96	3.02	3.06	3.09
LNP Size (DLS) (nm)	66	74	66	74	90	65
LNP Polydispersity (DLS)	0.169	0.331	0.207	0.286	0.356	0.162

a. T0 is shared for 2-8 °C and 25 °C
Abbreviations: EFVP = essentially free of visible particulates; LNP = lipid nanoparticle; DLS = dynamic light scattering

Table 3.2.P.2.2-11. **Liquid Stability of BNT162b1 at 25 °C for 10 days including 3x Freeze and Thaw at 10 Days**

Quality Attribute	T0[a]	1 day	2 days	3 days	7 days	10 days	10 days (3X F/T)
Appearance (Color)	≤Y4	≤Y5	≤Y5	≤Y5	≤Y5	≤Y4	≤Y4
Appearance (Clarity)	>REF IV	>REF IV	>REF IV	>REF IV	>REF IV	>REF IV	>REF IV
Visible Particles	EFVP	EFVP	EFVP	EFVP	EFVP	EFVP	EFVP
pH	6.9	NT	NT	6.9	NT	6.9	6.8
RNA Content (Ribogreen) (µg/mL)	432	438	442	458	436	434	450
RNA Encapsulation (Ribogreen) (%)	91	91	91	91	91	90	88
ALC-0315 Content (mg/mL)	7.92	7.22	7.24	7.40	7.21	7.24	7.24
ALC-0159 Content (mg/mL)	0.96	0.87	0.87	0.90	0.85	0.87	0.85
DSPC Content (mg/mL)	1.67	1.55	1.55	1.58	1.46	1.46	1.45
Cholesterol Content (mg/mL)	3.36	3.06	3.04	3.09	3.02	3.04	3.02
RNA Integrity (FA) (%)	88	87	86	86	85	84	85
LNP Size (DLS) (nm)	66	66	70	67	73	65	88
LNP Polydispersity (DLS)	0.169	0.195	0.259	0.193	0.353	0.169	0.261

a. T0 is shared for 2-8 °C and 25 °C
Abbreviations: EFVP = essentially free of visible particulates; LNP = lipid nanoparticle; DLS = dynamic light scattering; NT = not tested

3.2.P.2.2.1.3.2. BNT162b2 Drug Product Development Stability

A development stability study has been initiated for BNT162b2 drug product. LNPs were fabricated and formulated in PBS, 300 mM sucrose, pH 7.4 in the Pfizer Andover development laboratory. The drug product was filled at 0.45 mL/vial in 2 mL vials. Vials were stoppered, capped and stored at -80 °C, -40±5 °C (-40 °C), -20±5 °C (-20 °C), 2-8 °C and 25±2 °C (25 °C) for up to 6 weeks. The study condition of -80 °C is supportive of a storage temperature range -90 °C to -60 °C.

Results of these studies using the BNT162b2 drug product indicate that there was no change to quality attributes related to LNP size, LNP polydispersity or % RNA encapsulation when the drug product was stored at -80 °C, representative of the recommended frozen storage temperature of -90 to -60 °C, for up to 6 weeks, and accelerated temperatures of 2-8 °C for up to 6 weeks and 25 °C for up to 4 weeks. When the BNT162b2 drug product was subjected to the accelerated frozen temperatures of -40 °C or -20 °C which are close to or above the T_g' of -38.8 °C (Section 3.2.P.2.2.3.3) there appeared to be a slight increase in LNP size at 7 days and 2 weeks, however this trend did not continue to the 4 week timepoint. These results are similar to the BNT162b1 results discussed in Section 3.2.P.2.2.1.3.1. This suggests that LNPs from the two constructs exhibit similar stability for these quality attributes. Hence, conclusions arising from studies performed with BNT162b1 can be applied to BNT162b2 as the frozen and accelerated data are similar for the two constructs.

BNT162b2 drug product stored frozen at -80 °C, -40 °C and -20 °C remained stable and all attributes showed no pattern related to storage conditions for these interim durations: 6 weeks at -80 °C, 4 weeks at -40 °C and 4 weeks at -20 °C.

At 2-8 °C, in vitro expression appeared to decrease at 4 weeks but was comparable to the control at 6 weeks, indicating the change observed is within assay variability. All other attributes were comparable to the 6-week timepoint. These results indicate that BNT162b2 drug product is stable for up to 6 weeks when stored at 2-8 °C.

When BNT162b2 drug product was stored at 25 °C, RNA integrity (%) was less than 50% at 2 weeks and 4 weeks. There was a decrease in in-vitro expression (%) that appeared to be related to time but as the internal assay control showed the same trend, this was likely due to assay variability. All other attributes were comparable to the T0 control. These results indicate that BNT162b2 drug product is stable for up to 10 days when stored at 25 °C.

Results are shown in Table 3.2.P.2.2-12, Table 3.2.P.2.2-13, Table 3.2.P.2.2-14, Table 3.2.P.2.2-15 and Table 3.2.P.2.2-16.

Table 3.2.P.2.2-12.   Frozen Stability of BNT162b2 at -80 °C for 6 Weeks

Quality Attribute	T0[a]	7 days	4 weeks	6 weeks
Appearance (Visible Particles)	EFVP	EFVP	EFVP	EFVP
pH	7.2	NT	7.3	7.2
RNA Content (Ribogreen) (mg/mL)	0.45	0.37	0.46	0.34
RNA Encapsulation (Ribogreen) (%)	93	91	96	95
ALC-0315 Content (mg/mL)	4.57	4.82	4.68	4.63
ALC-0159 Content (mg/mL)	0.59	0.60	0.60	0.60
DSPC Content (mg/mL)	1.00	1.03	1.01	0.98
Cholesterol Content (mg/mL)	1.97	2.09	2.05	2.03
LNP Size (DLS) (nm)	67	75	69	74
LNP Polydispersity (DLS)	0.3	0.2	0.2	0.2
Subvisible particles (≥ 25 μm)	56	0	NT	NT
Subvisible particles (≥ 10 μm)	1278	222	NT	NT
RNA Integrity (CE) (%)	64	61	61	61
5'-Cap (RP-HPLC) (%)	85	85	83	83
IVE (% cells positive 100 ng)	79	69	26	48
IVE (% cells positive 150 ng)	88	88	52	68
IVE Control (150 ng) (%)[b]	73	73	49	49
Poly(A) tail (ddPCR) (%)	94	88	95	90

a.   T0 shared for all timepoints
b.   IVE Control is stored at recommended frozen storage condition and not subjected to stability condition.
Abbreviations: EFVP = Essentially free of visible particulates; NT = Not tested; LNP = Lipid nanoparticle; DLS = Dynamic light scattering; CE = Capillary electrophoresis; RP-HPLC = Reversed phase HPLC; IVE = In vitro expression; ddPCR = Droplet digital PCR

Table 3.2.P.2.2-13.   Frozen Stability of BNT162b2 at -40 °C for Four Weeks

Quality Attribute	T0[a]	7 days	2 weeks	4 weeks
Appearance (Visible Particles)	EFVP	EFVP	EFVP	EFVP
pH	7.2	NT	7.2	7.2
RNA Content (Ribogreen) (mg/mL)	0.45	0.33	0.39	0.43
RNA Encapsulation (Ribogreen) (%)	93	90	93	96
ALC-0315 Content (mg/mL)	4.57	5.03	4.70	4.88
ALC-0159 Content (mg/mL)	0.59	0.62	0.60	0.62
DSPC Content mg/mL)	1.00	1.09	1.02	1.06
Cholesterol Content (mg/mL)	1.97	2.19	2.02	2.13
LNP Size (DLS) (nm)	67	79	81	78
LNP Polydispersity (DLS)	0.3	0.2	0.2	0.2
Subvisible particles ($\geq$ 25 μm)	56	0	0	0
Subvisible particles ($\geq$ 10 μm)	1278	167	556	389
RNA Integrity (CE) (%)	64	61	62	61
5'-Cap (RP-HPLC) (%)	85	85	85	83
IVE (% cells positive 100 ng)	79	75	63	56
IVE (% cells positive 150 ng)	88	86	69	69
IVE Control (150 ng) (%)[b]	73	73	54	49
Poly(A) tail (ddPCR) (%)	94	98	90	104

a.   T0 shared for all timepoints
b.   IVE Control is stored at recommended frozen storage condition and not subjected to stability condition.
Abbreviations: EFVP = Essentially free of visible particulates; NT = Not tested; LNP = Lipid nanoparticle;
DLS = Dynamic light scattering; CE = Capillary electrophoresis; RP-HPLC = Reversed phase HPLC; IVE = In
vitro expression; ddPCR = Droplet digital PCR

Table 3.2.P.2.2-14.   Frozen Stability of BNT162b2 at -20 °C for Four Weeks

Quality Attribute	T0[a]	7 days	2 weeks	4 weeks
Appearance (Visible Particles)	EFVP	EFVP	EFVP	EFVP
pH	7.2	NT	7.2	7.2
RNA Content (Ribogreen) (mg/mL)	0.45	0.36	0.39	0.33
RNA Encapsulation (Ribogreen) (%)	93	88	92	94
ALC-0315 Content (mg/mL)	4.57	4.97	4.53	4.87
ALC-0159 Content (mg/mL)	0.59	0.62	0.62	0.63
DSPC Content (mg/mL)	1.00	1.07	0.98	1.06
Cholesterol Content (mg/mL)	1.97	2.15	1.95	2.13
LNP Size (DLS) (nm)	67	89	92	74
LNP Polydispersity (DLS)	0.3	0.3	0.3	0.2
Subvisible particles ($\geq$ 25 μm)	56	0	0	0
Subvisible particles ($\geq$ 10 μm)	1278	722	333	334
RNA Integrity (CE) (%)	64	62	63	61
5'-Cap (RP-HPLC) (%)	85	85	85	83
IVE (% cells positive 100 ng)	79	82	65	66
IVE (% cells positive 150 ng)	88	91	75	70
IVE Control (150 ng) (%)[b]	73	73	54	49
Poly(A) tail (ddPCR) (%)	94	98	86	97

a.   T0 shared for all timepoints
b.   IVE Control is stored at recommended frozen storage condition and not subjected to stability condition.
Abbreviations: EFVP = Essentially free of visible particulates; NT = Not tested; LNP = Lipid nanoparticle;
DLS = Dynamic light scattering; CE = Capillary electrophoresis; RP-HPLC = Reversed phase HPLC; IVE = In
vitro expression; ddPCR = Droplet digital PCR

Table 3.2.P.2.2-15. **Liquid Stability of BNT162b2 at 2-8 °C for 6 Weeks**

Quality Attribute	T0[a]	5 days	10 days	2 Weeks	4 Weeks	6 weeks
Visible Particles	EFVP	EFVP	EFVP	EFVP	EFVP	EFVP
pH	7.2	7.2	7.2	7.2	7.2	7.2
RNA Content (Ribogreen) (mg/mL)	0.45	0.36	0.34	0.41	0.37	0.36
RNA Encapsulation (Ribogreen) (%)	93	92	94	95	96	94
ALC-0315 Content (mg/mL)	4.57	4.77	4.82	4.61	4.77	4.62
ALC-0159 Content (mg/mL)	0.59	0.58	0.61	0.63	0.62	0.61
DSPC Content (mg/mL)	1.00	1.03	1.04	1.00	1.03	0.98
Cholesterol Content (mg/mL)	1.97	2.07	2.09	1.98	2.08	2.01
LNP Size (DLS) (nm)	67	62	62	62	63	62
LNP Polydispersity (DLS)	0.3	0.2	0.2	0.2	0.2	0.2
Subvisible particles ($\geq 25 \, \mu m$)	56	0	0	56	0	0
Subvisible particles ($\geq 10 \, \mu m$)	1278	167	667	167	222	167
RNA Integrity (CE) (%)	64	60	59	60	58	56
5'-Cap (RP-HPLC) (%)	85	85	85	85	83	84
IVE (% cells positive 100 ng)	79	64	41	25	40	37
IVE (% cells positive 150 ng)	88	77	67	61	38	52
IVE Control (150 ng) (%)[b]	73	73	54	54	49	49
Poly(A) tail (ddPCR) (%)	94	98	99	90	92	85

a. T0 is shared for all timepoints
b. IVE Control is stored at recommended frozen storage condition and not subjected to stability condition.
Abbreviations: EFVP = Essentially free of visible particulates; NT = Not tested; LNP = Lipid nanoparticle;
DLS = Dynamic light scattering; CE = Capillary electrophoresis; RP-HPLC = Reversed phase HPLC; IVE = In
vitro expression; ddPCR = Droplet digital PCR

Table 3.2.P.2.2-16.   Liquid Stability of BNT162b2 at 25 °C for 4 Weeks

Quality Attribute	T0[a]	3 days	5 days	10 days	2 weeks	4 weeks
Visible Particles	EFVP	EFVP	EFVP	EFVP	EFVP	EFVP
pH	7.2	7.1	7.2	7.1	7.1	7.1
RNA Content (Ribogreen) (mg/mL)	0.45	0.33	0.35	0.32	0.40	0.31
RNA Encapsulation (Ribogreen) (%)	93	94	90	92	92	93
ALC-0315 Content (mg/mL)	4.57	4.83	4.77	4.89	4.60	4.83
ALC-0159 Content (mg/mL)	0.59	0.59	0.59	0.61	0.59	0.63
DSPC Content (mg/mL)	1.00	1.04	1.03	1.04	0.98	1.03
Cholesterol Content (mg/mL)	1.97	2.08	2.06	2.12	1.97	2.09
LNP Size (DLS) (nm)	67	65	62	66	65	74
LNP Polydispersity (DLS)	0.3	0.2	0.2	0.3	0.3	0.2
Subvisible particles (≥ 25 μm)	56	56	0	0	111	0
Subvisible particles (≥ 10 μm)	1278	445	556	834	445	722
RNA Integrity (CE) (%)	64	56	53	51	47	37
5'-Cap (RP-HPLC) (%)	85	85	85	85	85	84
IVE (% cells positive 100 ng)	79	64	68	48	38	36
IVE (% cells positive 150 ng)	88	81	75	68	56	47
IVE Control (150 ng) (%)[b]	73	73	73	54	54	49
Poly(A) tail (ddPCR) (%)	94	84	88	75	77	87

a.   T0 shared for all timepoints
b.   IVE Control is stored at recommended frozen storage condition and not subjected to stability condition.
Abbreviations: EFVP = Essentially free of visible particulates; NT = Not tested; LNP = Lipid nanoparticle;
DLS = Dynamic light scattering; CE = Capillary electrophoresis; RP-HPLC = Reversed phase HPLC; IVE = In
vitro expression; ddPCR = Droplet digital PCR

3.2.P.2.2.1.4. Frozen Stability of Drug Product

The BNT162b2 drug product is stored frozen at the recommended storage temperature of
-90 to -60 °C. Differential scanning calorimetry was performed on the BNT162b2 frozen
drug product, which exhibits two glass transition events characteristic of
saccharide-containing formulations with onset temperatures at -51.8 °C ± 0.8 °C and
-38.8 °C ± 0.1 °C. The higher temperature event, Tg', is identified as the glass transition of
the maximally freeze-concentrated solution. Molecular mobility decreases below the glass
transition which prevents instability over time. Based on an understanding of the glassy state
dynamics and available stability data for the BNT162b1 drug product stored at -70 ± 10 °C as
shown in Table 3.2.P.2.2-8 and available stability data for BNT162b2 drug product stored
frozen as shown in Table 3.2.P.2.2-12, instability at temperatures below -60 °C is not
expected.

Studies addressing the frozen stability of BNT162b2 are ongoing. See Section 3.2.P.8.3 Long
Term.

3.2.P.2.2.1.5. Excess Volume in Vial

The target fill volume for 225 μg/vial BNT162b2 drug product is 0.45 mL. Since the drug
product is intended for multiple doses, the vial contents are diluted with 1.8 mL sterile 0.9%
sodium chloride for injection (normal saline) for a total dosing solution volume of 2.25 mL.
In addition to the volume necessary to supply 5 doses (0.3 mL each for a total of 1.5 mL)

there is an excess volume of 0.75 mL ensuring that five doses can be removed from the vial and delivered.

An initial study was performed with BNT162b1 to determine the hold-up volume in the 2 mL stoppered vial. In the absence of data for the BNT162b2 drug product, results for BNT162b1 filled into the same vial with the same fill volume are shown here to provide a reasonable assessment of the volume requirements for BNT162b2 drug product due to the equivalency of their solution properties. The study design is briefly described:

- 8 empty vials, with stopper and crimp seal were weighed.
- Vials were filled with 0.45 mL of BNT162b1 drug product.
- Vials were crimped and sealed and then weighed.
- 1.8 mL of normal saline was added to each vial.
- Diluted vials, including stopper and crimp seal, were weighed.
- 5 x 0.3 mL volumes were separately withdrawn from each vial through the stopper into 1 mL syringes with 23 G 1-inch needles.
- Emptied vials containing residual and hold-up volume were weighed.
- Residual volume was withdrawn from each vial.
- Emptied vials containing hold-up volume were weighed.
- The 5 withdrawn doses from each vial were ejected from the syringe and weighed.

Results of the extractable volume study indicated that an average of 2.09 mL could be withdrawn from the vial. The average hold-up volume in the vial was 0.12 mL (Table 3.2.P.2.2-17).

The delivered injection volume study shows that an average of up to 1.65 mL can be delivered over 5 separate injections with separate 1 mL syringes. No vial had a total delivered injection volume of less than 1.5 mL (Table 3.2.P.2.2-18).

The difference between the extractable volume from the vial (Withdrawn Solution in Table 3.2.P.2.2-17) and the delivered dose volume (Total Delivered Injection Volume in Table 3.2.P.2.2-18) is due to the hold-up volume of the 5 dosing syringe and needle assemblies.

Based on this study, the chosen fill volume of 0.45 mL and the excess volume of 0.75 mL after dilution with 1.8 mL normal saline is appropriate for delivering 5 doses of 0.3 mL from the BNT162b2 multi-dose vial.

Table 3.2.P.2.2-17.   Extractable Volume and Hold-up Volume of BNT162b1 Drug Product with Dilution in Normal Saline and Extraction of Five Doses

Vial No.	Weight (g)				
	Dosing Solution	Extracted Solution for 5 Doses	Extractable Residual	Vial Hold-up	Total Extractable
1	2.255	1.949	0.194	0.112	2.143
2	2.237	1.952	0.149	0.136	2.101
3	2.229	1.912	0.195	0.122	2.107
4	2.211	1.921	0.197	0.093	2.118
5	2.229	1.932	0.156	0.141	2.088
6	2.217	2.031	0.072	0.114	2.103
7	2.257	1.912	0.226	0.119	2.138
8	2.231	1.958	0.176	0.097	2.134
Average	**2.231**	**1.990**	**0.171**	**0.117**	**2.119**
	Volume (mL)				
Weight/ (1.0122 g/mL)[a]	2.204	1.966	0.169	0.115	2.093

a.   Density of the diluted solution is 1.0122 g/mL

Table 3.2.P.2.2-18.   Delivered Injection Volume over 5 Separate Injections with 1 ml Syringes

Vial No.	A	B	C = A + B	D = C/(1.0122 g/mL)[a]
	Sum of 5 Doses per Vial (g)[b]	Extractable Additional Content (g)	Total Deliverable (g)	Total Deliverable Volume (mL)
1	1.499	0.194	1.693	1.67
2	1.508	0.149	1.657	1.64
3	1.499	0.195	1.694	1.67
4	1.523	0.197	1.720	1.70
5	1.521	0.156	1.677	1.66
6	1.519	0.072	1.591	1.57
7	1.471	0.226	1.697	1.68
8	1.486	0.176	1.662	1.64
Average	**1.503**	**0.171**	**1.674**	**1.65**

a.   Density of the diluted solution is 1.0122 g/mL
b.   Sum of 5 doses drawn up into 5 syringe and needle assemblies, ejected and weighed for each vial

3.2.P.2.2.2. Overages

No overage has been added to BNT162b2 drug product.

3.2.P.2.2.3. Physicochemical and Biological Properties

In alignment with ICH Q8, the physicochemical and biological properties of BNT162b2 drug product relevant to the safety, performance and manufacturability of the drug product have been identified and appropriately characterized or controlled (Section 3.2.P.5.1 Specifications).

3.2.P.2.2.3.1. Density

The density of the BNT162b2 drug product has been measured as 1.04 g/mL at 20 °C.

3.2.P.2.2.3.2. Viscosity

The viscosity of the drug product is 1.42 cP measured at 20 °C, 0.5 mg/mL.

3.2.P.2.2.3.3. Thermal Transitions

Differential scanning calorimetry was performed on the BNT162b2 frozen drug product, which exhibits two glass transition events characteristic of saccharide-containing formulations with onset temperatures at -51.8 °C ± 0.8 °C and -38.8 °C ± 0.1 °C. The higher temperature event, Tg', is identified as the glass transition of the maximally freeze-concentrated solution.

3.2.P.2.2.3.4. Enhanced Analytical Characterization

This section will describe the structure and other physicochemical properties for BNT162b2 drug product as assessed through enhanced analytical characterization as outlined in Table 3.2.P.2.2-19.

Table 3.2.P.2.2-19.   Enhanced Characterization Strategy for Physicochemical Properties of BNT162b2 Drug Product

Physicochemical Properties	Analytical Approach	Methodology
RNA Integrity	Electrophoretic separation of RNA following LNP disruption	Capillary Gel Electrophoresis
Size distribution and particle shape	Hydrodynamic separation of particles	Asymmetric Flow Field Flow Fractionation-Multi-Angle-Light-Scattering-Quasi-Elastic-Light-Scattering (AF4-MALS-QELS)
Surface charge	Zeta potential analysis	Electrophoretic Light Scattering
Surface PEG	Spectroscopic analysis	1-Dimensional Proton Nuclear Magnetic Resonance (NMR) Spectroscopy

3.2.P.2.2.3.4.1. RNA Integrity

The RNA integrity of BNT162b2 drug product samples is assessed using a capillary gel electrophoresis-based (CGE) method, also called the Fragment Analyzer (FA) method, to separate components based on the differential migration of RNA of different molecular size in an applied electric field. In contrast to drug substance sample analysis, RNA from drug product is analyzed following disruption of the LNP in detergent and ethanol. Under fully denaturing conditions, the RNA is expected to unfold and migrate through the gel matrix, as a function of length and size, toward the anode. An intercalating dye binds to RNA and associated fragments during migration allowing for fluorescence detection. All other peaks that migrate prior to or after the main peak are integrated separately and will lower the overall RNA integrity percent, ie. intact RNA. The efficacy of the product is dependent on expression of the delivered RNA, which requires a sufficiently intact RNA molecule.

In general, three main species are observed in the RNA integrity assay by CGE: fragments, main, and those species that migrate later than the main peak. The species that migrate after the main peak are observed in recent drug product batches and are typically not present in the final mRNA drug substance. Although fragments are consistently observed between drug substance and drug product, further characterization of the composition of the late-migrating species (LMS) was undertaken to confirm the composition of the LMS as RNA.

Characterization results from the evaluation by multiple techniques demonstrate the LMS is indeed intact RNA. An orthogonal separation (ion pairing reverse phased HPLC) that separated late eluting species that correlate with the presence of LMS was used. MALS data showed the peak represented a size consistent with the main peak. Mass spectrometry (MS) characterization of the enzymatically digested RNA to form nucleosides and nucleotides confirmed the presence of expected nucleosides/nucleotides and no significant modifications to the RNA greater than 0.1% or different from DS. MS/MS data confirm no unexpected modifications to the four RNA bases. The LMS is therefore characterized as conformationally folded or reversibly aggregated RNA that is not denatured in the CGE method. A summary of the characterization results is provided in Table 3.2.P.2.2-20.

Table 3.2.P.2.2-20.   Characterization of Late-Migrating Species (LMS) Observed by CGE

Analytical Technique	Purpose	Results
RNase Treatment Followed by FA	Determine if FA LMS is RNA	• RNase treatment eliminates main peak, fragments, and LMS. LMS is comprised of RNA.
Ion Pairing RP-HPLC	Evaluate RNA extracted from LNP by an orthogonal RNA separation method more amenable to characterization. Characterize collected peaks by FA, IP-RP-HPLC reinjection, denaturing agarose gel electrophoresis (AGE) and multi-angle light scattering (MALS).	• RNA species can be separated, and fractions can be collected by RP-HPLC. Late-eluting peaks observed, abundance correlated with LMS levels. • Late-eluting peaks showed as intact RNA by denaturing AGE. • One of the late-eluting peaks (peak 3) runs as intact RNA by FA; another late-eluting peak (peak 5) also contains intact RNA by FA although some level of LMS is maintained in that fraction. • Late-eluting peaks consistent with intact RNA by MALS.
Nucleoside/nucleotide analysis by mass spectrometry	Characterization of individual nucleosides and nucleotides of RNA from drug product, as well as fractions collected from IP-RP-HPLC	• The LC-MS/UV results demonstrate that BNT162b2 mRNA contains the intended nucleosides/nucleotides. No significant level of modified residues was detected, especially considering the ability of the method to detect the single guanosine with the 5'-Cap moiety.

An electropherogram of lot EG5411, an engineering run that demonstrated the presence of fragments, main intact RNA and LMS peaks, is shown in Figure 3.2.P.2.2-6. The LMS

migrates to the right of the main intact RNA species. The composition of the LMS was confirmed to be RNA by treating the sample with RNase A prior to analysis by FA.

Figure 3.2.P.2.2-6.   Fragment Analyzer Profile of EG5411 Before and After RNase A Treatment
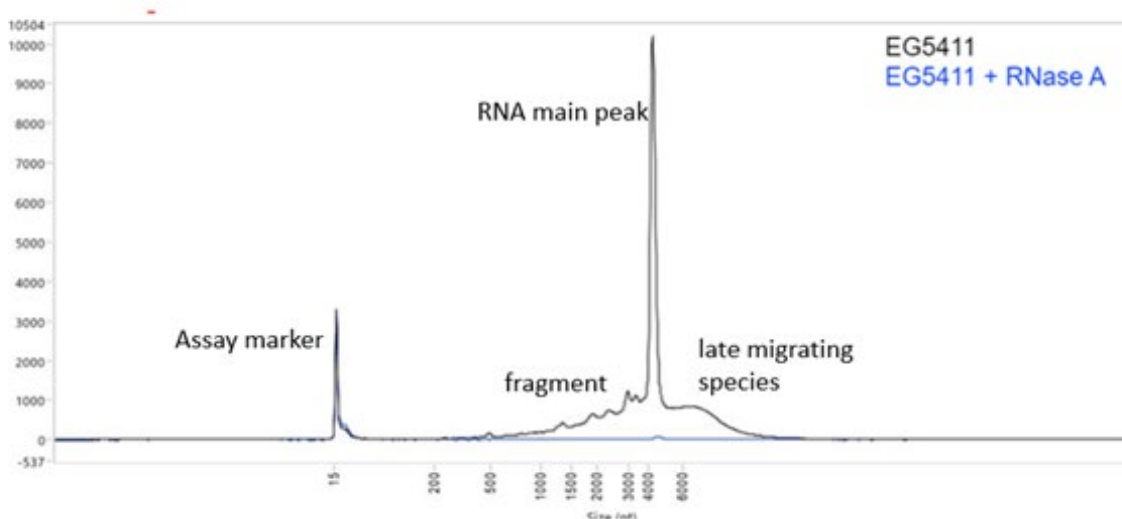
An ion-pairing reversed phase-HPLC method was used as an orthogonal method to separate RNA after extraction from the drug product sample. The IP-RP-HPLC method elutes different RNA species using a gradient of methanol containing hexafluoroisopropanol (HFIP) and triethylamine (TEA), followed by a "strip" elution using 50% methanol/30% isopropanol, with UV detection at 260 nm. To facilitate further characterization of the IP-RP-HPLC peaks, peaks 1-5 were collected from multiple injections of extracted DP lots, partially dried down, pooled, and dried down further to a volume of suitable concentration. Peak 4, which is only present at a very low level, was not individually collected but collected in a group with the other late-eluting peaks, 3 and 5. The collected fractions were reinjected onto IP-RP-HPLC to verify purity.

Figure 3.2.P.2.2-7.   IP-RP-HPLC Profile of Extracted RNA and Isolated Fractions
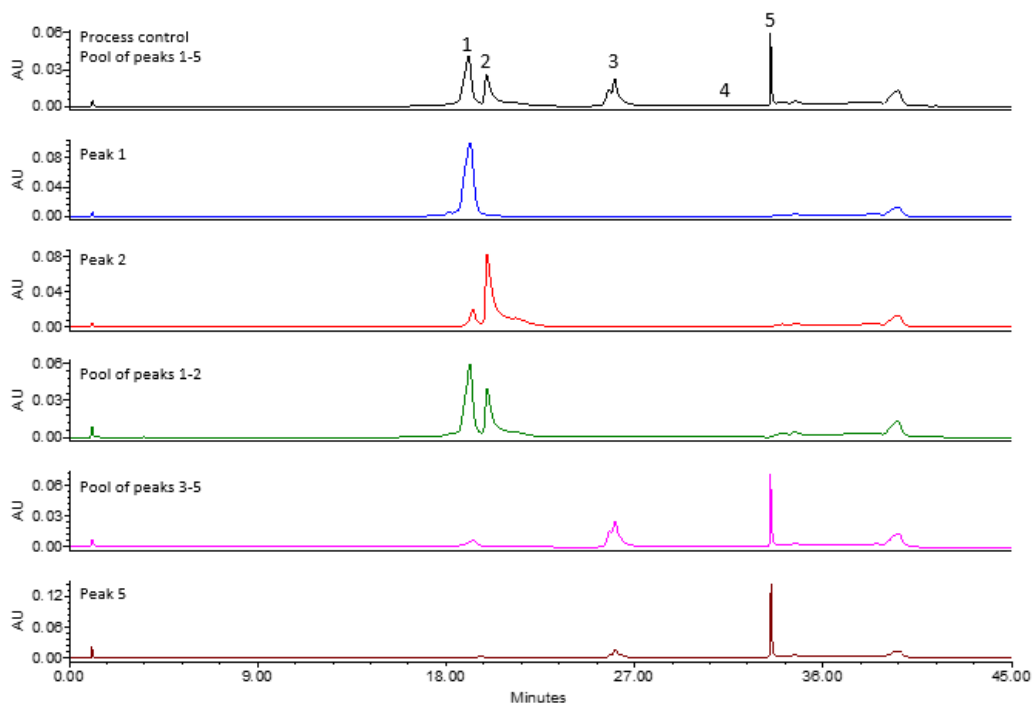
IP-RP-HPLC was coupled with online MALS analysis to determine the apparent size of the various peaks (Figure 3.2.P.2.2-8). The molar mass (left panel) and root mean square (RMS) radius (right panel) of the late-eluting species were all similar to that of Peak 1 or Peak 2, which correspond to fragment or intact RNA species, respectively. Notably, there is no evidence of any RNA species in any of the peaks including peak 5 that are larger in size than the intact RNA in Peak 2.

Figure 3.2.P.2.2-8.   IP-RP-HPLC MALS of RNA Extracted from DP Lot EG5411
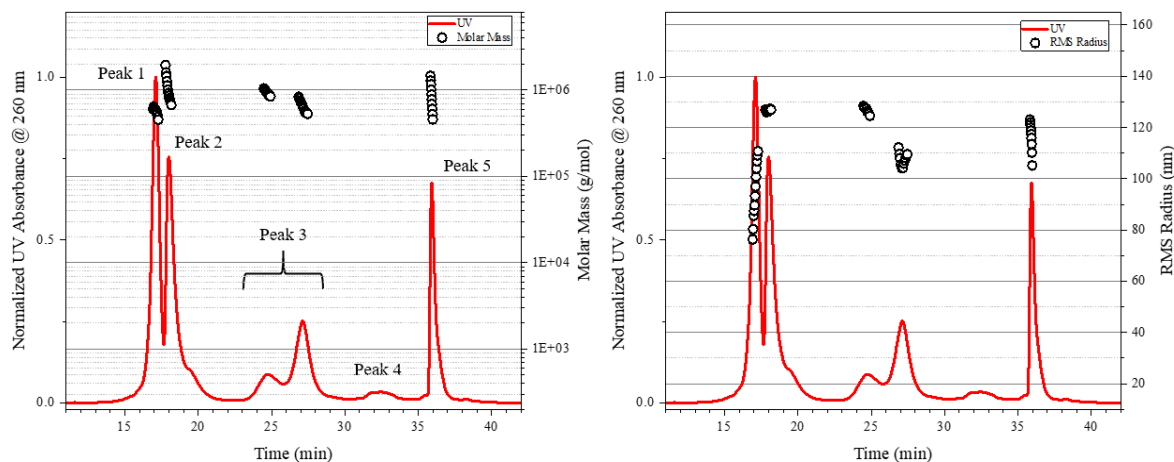
Fractionated IP-RP-HPLC peaks were also analyzed by denaturing agarose gel electrophoresis (AGE) that uses sample loading buffer containing formamide and

formaldehyde, and agarose gel containing formaldehyde. Peak 1 is RNA fragments, all other fractions were consistent in apparent size to the process control (isolation of all peaks in one sample) and to the main (intact) band in extracted, unfractionated RNA from a number of DP samples (Figure 3.2.P.2.2-9). Peak 5 was also confirmed by fully denaturing agarose gel electrophoresis (AGE) to be the same size as intact RNA.

Figure 3.2.P.2.2-9. **Denaturing AGE of Extracted RNA from DP Lots and of IP-RP-HPLC Fractions from DP Lot EG5411**
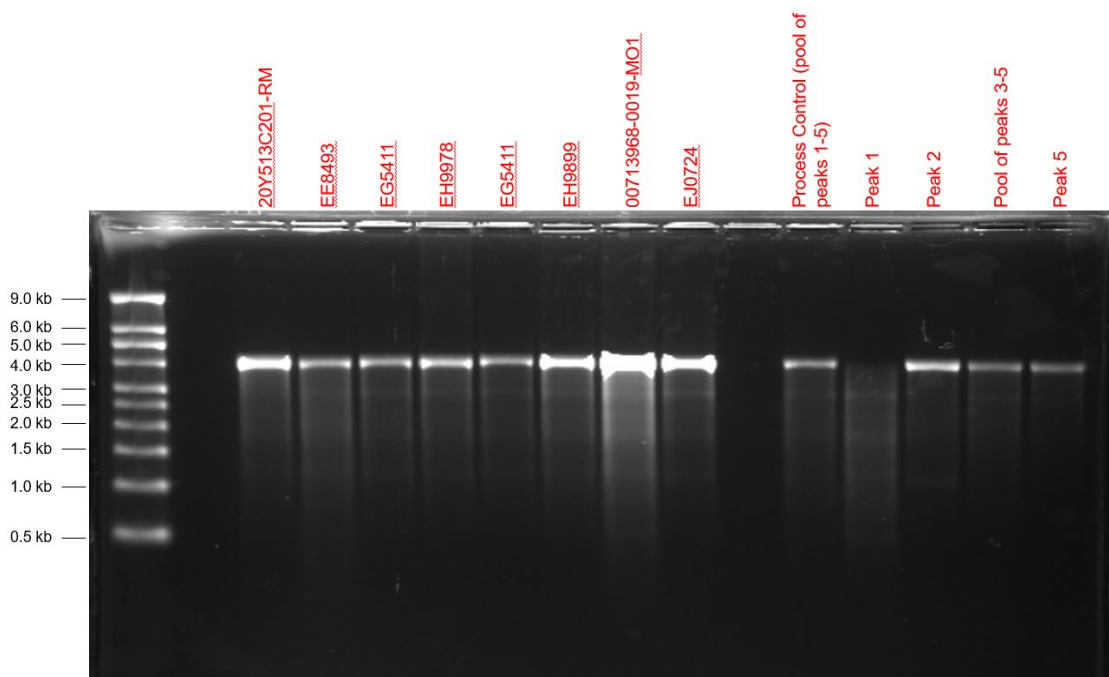
EE8493 is a clinical lot. EE8493, EH9899, EJ0724 are intended emergency supply lots pending disposition. EG5411 and EE9978 are engineering runs. 20Y513C201-RM is a drug substance control. 007133968W19-M01 is a lab scale lot. Peaks 1-5 were isolated by IP-RP-HPLC as noted above from lot EG5411.

The individual nucleosides and nucleotides of BNT162b2 were characterized by LC-UV-MS analysis following mRNA hydrolysis. To generate nucleotides, nuclease P1 and venom phosphodiesterase were used at low and high pH, respectively, to hydrolyze the phosphodiester bonds of RNA, which keeps the phosphate group intact. To generate nucleosides, the procedure is identical except for the addition of alkaline phosphatase to remove the phosphate group, leaving the ribose and nucleobase for adenosine (A), guanosine (G), N1-methyl-pseudouridine (V) and cytidine (C).

The nucleotide and nucleoside LC-UV-MS/MS analysis was conducted on the individual collected peak fractions derived from lot EG5411 (i.e., the extracted DP lot where higher levels of LMS were observed), as well as two controls: bulk, unfractionated DP EG5411 and a process control comprising peak fractions 1-5 (i.e., individual collected fractions were partially vacuum dried and then recombined back into a single sample). The resulting nucleotide and nucleoside UV chromatograms, in Figure 3.2.P.2.2-10 and Figure 3.2.P.2.2-11, respectively, show complete, consistent digestion of all collected peak fractions,

including peak 5, after employing the following digest conditions: 10 min denaturation at
95 °C, nuclease P1 digestion for 1-hour at 55 °C, and phosphodiesterase for 1-hour at 37 °C.

**Figure 3.2.P.2.2-10.   LC-UV (A260 nm) Nucleotide Analysis of Peak Fractions 1-5 from
IP-RP-HPLC using Extracted DP Lot EG5411**

Figure 3.2.P.2.2-11.   LC-UV (A260 nm) Nucleoside Analysis of Peak Fractions 1-5 from IP-RP-HPLC using Extracted DP Lot EG5411

C   V   A   G   Peak 1

Peak 2

Peak 3

Peak 4

Peaks 3-5

Peak 5

20Y513C201 RM

EG5411

The LC-UV/MS results demonstrate that BNT162b2 mRNA contains the expected nucleosides/nucleotides, as well as the single 3′-O-methylated guanosine and 2′-O-methylated adenosine in the extended 5′-Cap structure. No additional modified residues greater than 0.1% were detected in the bulk DS and extracted bulk DP lots which is important given the sensitivity of the method to detect the two single O-methylated nucleosides within the 5′-Cap moiety.

In addition to the enhanced characterization data, Table 3.2.P.2-21 below summarizes the clinical trial material (CTM) and intended Emergency Supply (post-CTM) BNT162b2 lots with completed IVE results; RNA integrity and the IVE release assay data are shown. The lots EJ0701, EH9899, and EJ1688 had observable late migrating species. This was integrated separately from the main species therefore the RNA integrity represents only the main RNA peak area. The data show that CTM as well as post-CTM lots, while displaying some heterogeneity in the RNA integrity profile, demonstrate comparable IVE, which ensures similar efficacy. In vitro expression has been shown to correlate with antigen-binding antibody responses and SARS-CoV-2 neutralizing responses in mice immunized with the drug product (Section 3.2.P.2.2.1.1.3).

Table 3.2.P.2-21.   Drug Product RNA Integrity and In Vitro Expression Results

Drug Product Lot Number	Usage	ALC-0315 Source	RNA Integrity [a]	In Vitro Expression (percent positive cells, 150 ng)
BCV40420-A	CTM	Avanti	75%	69%
BCV40620-A	CTM	Avanti	85%	59%
BCV40620-D	CTM	Avanti	77%	71%
BCV40620-E	Development Material	Avanti	85%	67%
BCV40720-A	CTM	Avanti	71%	63%
BCV40720-P (ED3938)	CTM	Avanti	62%	50%
BCV40820-P (EE3813)	CTM	Avanti	63%	62%
EE8492	Post-CTM	Avanti	55%	63%
EE8493	CTM and Post-CTM [b]	Avanti	55%	65%
EJ0701	Post-CTM	Croda	52%	62%
EJ0724	Post-CTM	Avanti	71%	60%
EJ0553	CTM and Post-CTM [b]	Avanti	68%	62%
EH9899	Post-CTM	Croda	59%	49%
EJ1688	Post-CTM	Croda	63%	72%

a. RNA integrity is the %intact RNA. Fragment and late migrating species are integrated separately and lower the reported RNA integrity percent.
b. Lot included in clinical trial and also intended for Emergency Supply.
Abbreviation: CTM = clinical trial material

3.2.P.2.2.3.4.2. Size Distribution and Particle Shape

BNT162b2 drug product samples were analyzed by AF4-MALS-QELS in 1x PBS to characterize both particle size distribution and shape. Figure 3.2.P.2.2-12 shows that BNT162b2 drug product LNP exhibits a narrow hydrodynamic radius (Rh) distribution predominantly between 30 and 41 nm (Table 3.2.P.2.2-22). The overall ratio between root mean square radius and hydrodynamic radius (Rz/Rh) describes the shape of the particle. For BNT162b2, the average Rz/Rh ratio is 0.71, which is very close to the value of 0.77 for a solid spherical particle. The distribution of Rz/Rh ratio across the main peak also suggests that LNP with different sizes are still in similar spherical shape (Table 3.2.P.2.2-22). The AF4-MALS-QELS results indicate that BNT162b2 drug product has a relatively homogeneous size distribution and is largely spherical as expected.

Figure 3.2.P.2.2-12.   AF4-MALS-QELS Fractogram of BNT162b2 Drug Product
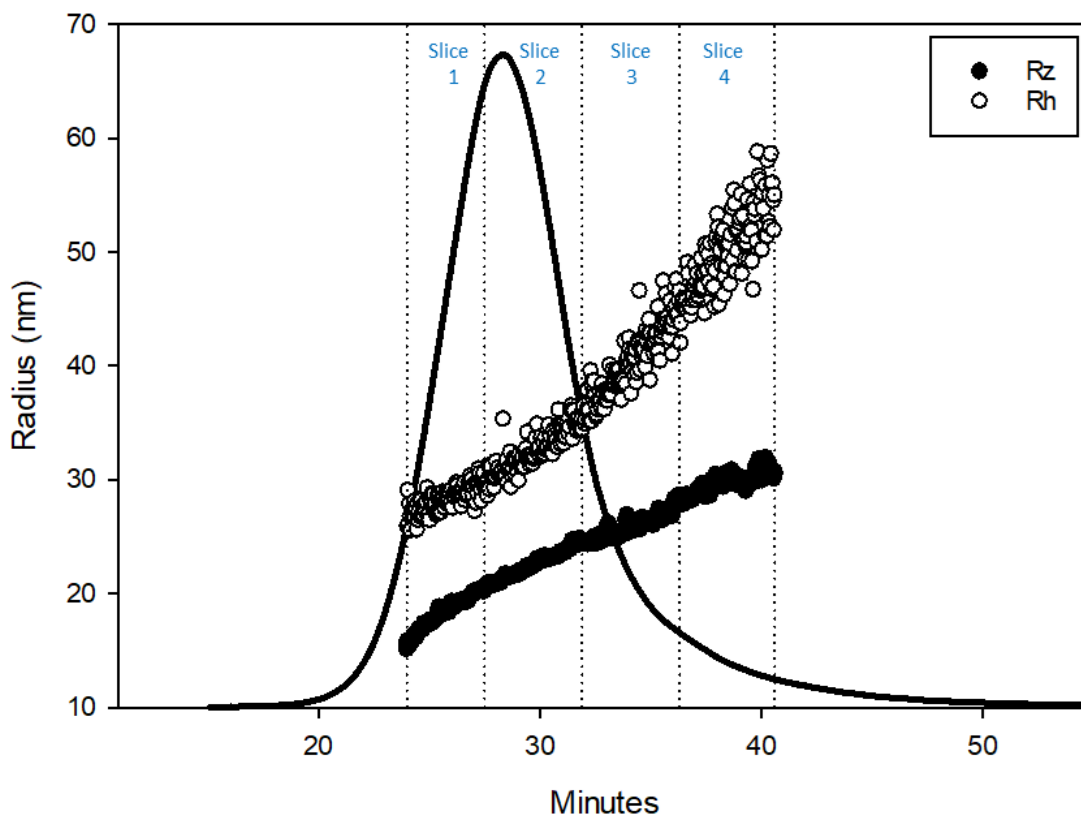
Table 3.2.P.2.2-22.   BNT162b2 Drug Product Size and Shape Distribution

Rh across elution profile (nm)				Rz/Rh across elution profile				Average Rz/Rh
Slice 1	Slice 2	Slice 3	Slice 4	Slice 1	Slice 2	Slice 3	Slice 4	0.71
30	33	41	51	0.67	0.70	0.65	0.60	

3.2.P.2.2.3.4.3. Particle Surface Charge

BNT162b2 drug product was subjected to electrophoretic light scattering analysis to determine the zeta potential, which is defined as the electrostatic potential between the particle surface and the bulk solvent. Figure 3.2.P.2.2-13 shows the zeta potential distribution for BNT162b drug product, which is narrow and monomodal. The average apparent zeta potential for BNT162b2 drug product is around -3.13 mV, indicating the surface of the LNP is slightly negatively charged. The nearly neutral LNP surface supports the mechanism that BNT162b2 drug product avoids non-specific binding events in the blood compartment as described in Section 3.2.P.2.2.1.1.

Figure 3.2.P.2.2-13. Zeta Potential Distribution of BNT162b2 Drug Product
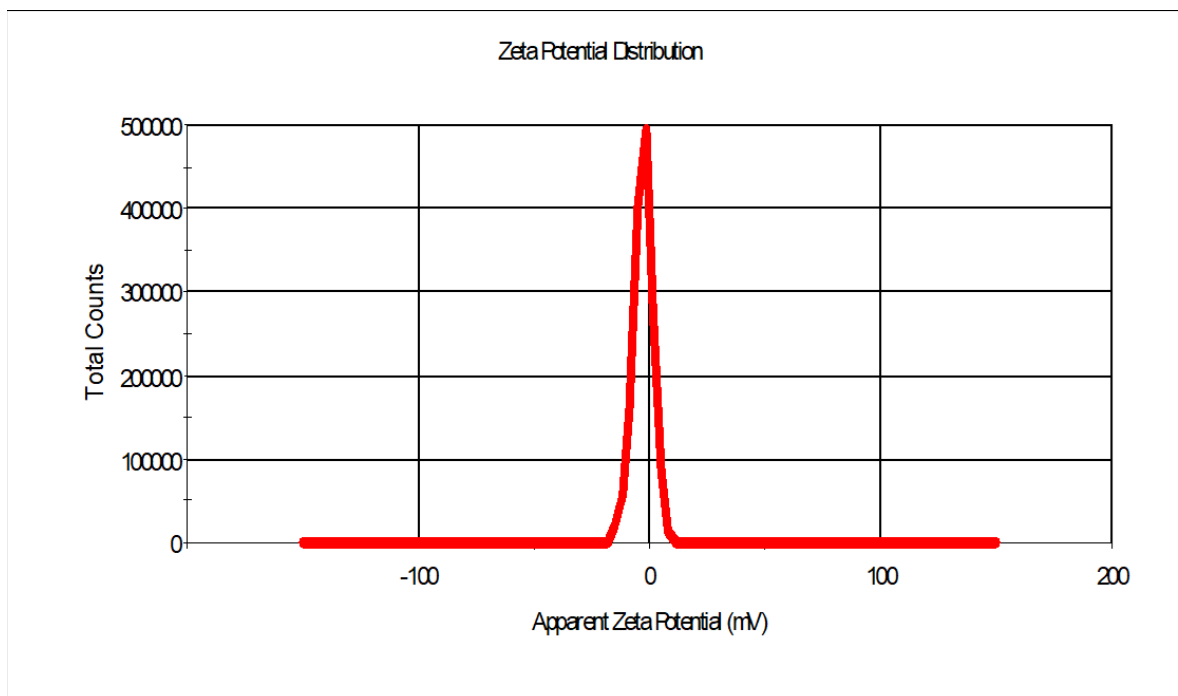
A diffusion barrier method was used to avoid particle degradation during analysis. The data collection was done in 0.1 x PBS pH 7.4 solution. The electrophoretic mobility was converted to zeta potential using Smoluchowski approximation to Henry's function provided by the instrument software.

3.2.P.2.2.3.4.4. Surface PEG of ALC-0159

An ultra-high field (800 MHz) NMR spectrometer was used to characterize the surface characteristics of the LNP. BNT162b2 DP was dialyzed into 0.2 x PBS with 10% D_2O to remove sucrose and the resulting BNT162b2 DP 1D proton NMR spectrum is presented in Figure 3.2.P.2.2-14, along with 1D proton NMR spectra of the individual LNP components for confirming peak assignments. NMR readily detected the protons associated with the PEG moiety of ALC-0159 at the surface of LNP due to the flexibility of PEG chains. A major peak at 3.71 ppm is associated with the multiple methylene protons of PEG repeating unit (n=45-50) and a smaller but distinctive peak at 3.39 ppm is from PEG terminal methyl group. The NMR peak assignments and intensity data confirms that PEG moiety from the functional ALC-0159 lipid is present at LNP surface in the BNT162b2 drug product samples. 1D proton NMR analysis also detected the presence of ALC-0315, the other functional lipid, near the surface from the methylene groups of the hydroxylbutyl group at 3.50 ppm and 2.29 ppm, respectively. In addition, the alkyl chains that are common to both ALC-0159 and ALC-0315 lipids are also detected near the surface. The signals for the alkyl chains are strong due to the large number of protons for each alkyl chain. 1D proton NMR signals from DSPC and cholesterol are not observed, suggesting that they are much less mobile and more tightly associated with the LNP as structural lipids. The 1D proton NMR results are consistent with the proposed LNP architecture and structure, particularly with the presence of surface PEG being supportive of the *in vivo* fate of BNT162b2 drug product in terms of ApoE-dependent cellular uptake. The detection of hydrophilic head of ALC-0315 at the LNP surface is also

consistent with the proposed dual roles of this functional lipid, which allows LNP becoming positively charged in low pH environment to favorably interact with endosomal membrane during endosome escape (see Section 3.2.P.2.2.1.1).

Figure 3.2.P.2.2-14.   1D Proton NMR Spectrum of BNT162b2 Drug Product (EE8493) and Individual Lipids
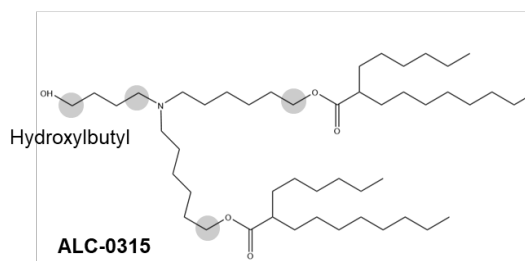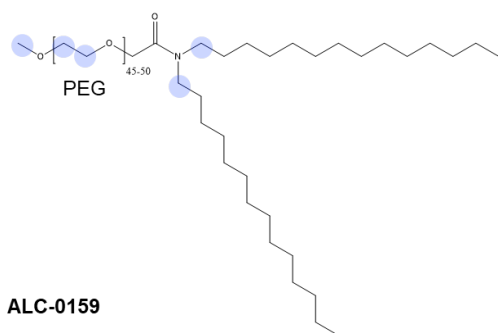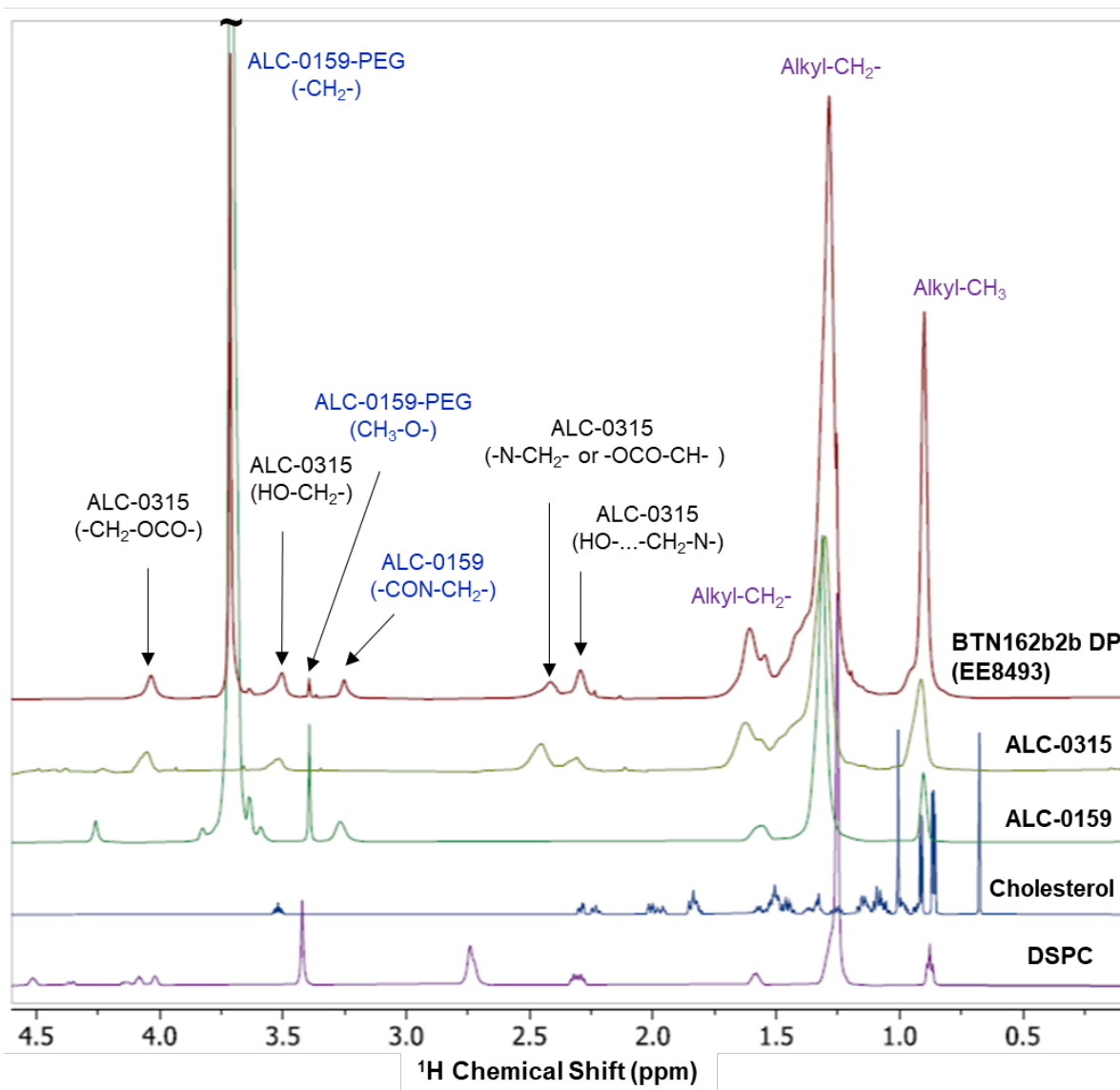
Figure 3.2.P.2.2-14: 1D Proton NMR spectra of BNT162b2 drug product (intact LNP), ALC-0159 and ALC-0315 were collected at 800 MHz in 0.2 x PBS, 10% D_2O using trimethylsilylpropanoic acid (TSP) as the

internal standard. Additional 1D Proton NMR spectra of cholesterol and DSPC were collected in chloroform-*d* with tetramethylsilane (TMS) as the internal standard due to their low solubility in aqueous solution. Chemical shift peaks labeled with blue annotation originate from ALC-0159 whereas the black annotated peaks are from ALC-0315. The chemical shift peaks in purple are common to both ALC-0315 and ALC-0159. Surface protons that are detected and specific to either ALC-0159 or ALC-0315 are also marked with circles in the respective chemical structures. The peak assignments are based on proton chemical shift prediction software, ACD LAB.

3.2.P.2.2.3.5. Appearance and Characterization of Intrinsic Particles

During the visual inspection step of the drug product manufacturing process, white colored particulate matter has been occasionally observed. Particulate matter was isolated by vacuum filtration onto 10 µm (pore size) gold filters, then imaged and analyzed using FTIR. Visible particulates are white in color, amorphous in shape, and of variable size as they tend to agglomerate. FTIR spectra for the particles were collected and compared to spectra of the LNP components using component analysis. From the component analysis, Figure 3.2.P.2.2-15, the highest match to the particulate matter came from a combined spectra including lipid components as well as a contribution from RNA.

Figure 3.2.P.2.2-15.   Comparison of FTIR Spectra for Intrinsic Particulate Matter and LNP Components
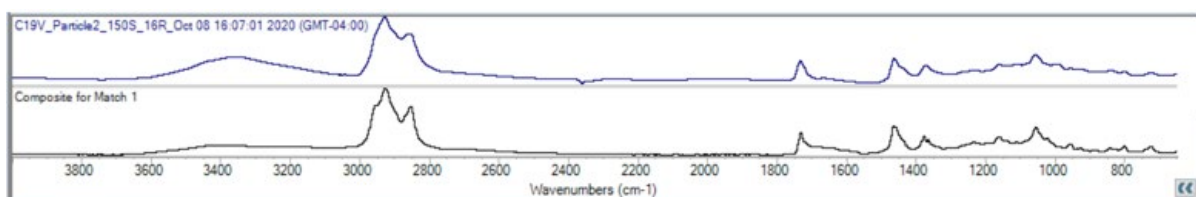
FTIR result from component analysis comparing spectra from a particulate from vial 1 to a composite spectra of lipid and RNA components.

These data indicate that the particulate matter is intrinsic to the product formulation. Agglomerated particulate matter appears to be dispersed upon addition of sterile 0.9% sodium chloride for injection and mixing as part of the dose preparation process.

3.2.P.2.2.4. Conclusions

A formulation for the 225 µg/vial BNT162b2 drug product, including four lipids to form RNA-containing lipid nanoparticles formulated in phosphate-buffered saline and 300 mM sucrose at pH 7.4, has been developed and has been shown to be appropriate for intramuscular administration.

Though stability studies are ongoing, based on available information, the drug product formulation is expected to meet the objectives of the drug product development and the quality target product profile described in Section 3.2.P.2 Introduction when manufactured with the commercial drug product process and stored at the recommended storage condition of -90 to -60 °C.

No overage is included in the drug product. There is an excess volume of 0.75 mL in the vial after dilution with 1.8 mL of sterile 0.9% sodium chloride to account for hold-up volume in the vial and provide the appropriate volume for removing 5 doses from the multi-dose vial.

Enhanced analytical characterization supports that the RNA-containing lipid nanoparticles in BNT162b2 drug product are relatively homogeneous in size and largely spherical in shape as expected. In addition, the nearly neutral particle surface and the presence of PEG moiety of ALC-0159 at the particle surface confirm the architecture and structure of the lipid nanoparticles. Characterization results from the evaluation by multiple techniques demonstrate the late migrating species (LMS) observed by capillarity gel electrophoresis is intact RNA. Lastly, particulate matter observed in drug product is consistent with LNPs by FTIR, indicating that the particulates are intrinsic to the product.

[1]   Semple S, Akinc A, Chen J, et al. Rational design of cationic lipids for siRNA delivery. 2010. Nature Biotechnology; 28:172-176.

[2]   Akinc A, Querbes W, De S, et al. Targeted Delivery of RNAi Therapeutics With Endogenous and Exogenous Ligand-Based Mechanisms. 2010. Mol Ther; 18(7): 1357-64.

[3]   Silvius J, Zuckermann M. Interbilayer Transfer of Phospholipid-Anchored macromolecules via monomer diffusion. 1993. Biochemistry; 32: 3153-3161.

[4]   Jayaraman M, Ansell S, Mui B, et al. Maximizing the Potency of siRNA Lipid Nanoparticles for Hepatic Gene Silencing In Vivo. 2012. Angew. Chem. Int. Ed; 51, 8529 –8533.

[5]   Rejman J, Oberle V, Zuhorn IS, et al. Size-dependent internalization of particles via the pathway of clathrin and caveolae-mediated endocytosis. Biochem. J. 2004. 377, 159-169.

[6]   Xie X, Muruato A, Lokugamage KG, et al. An infectious cDNA clone of SARS-CoV-2. Cell Host Microbe 2020; 27(5):841-848.e3.

[7]   Muruato AE, Fontes-Garfias CR, Ren P, et al. A high-throughput neutralizing antibody assay for COVID-19 diagnosis and vaccine evaluation. Nat Commun 2020;11(1):4059.